

The role of local orography on the development of a severe rainfall event over western Peninsular Malaysia: a case study

Article

Accepted Version

Mohd Nor, M. F. F., Holloway, C. E. ORCID: <https://orcid.org/0000-0001-9903-8989> and Inness, P. M. ORCID: <https://orcid.org/0009-0005-5795-6841> (2020) The role of local orography on the development of a severe rainfall event over western Peninsular Malaysia: a case study. *Monthly Weather Review*, 148 (5). pp. 2191-2209. ISSN 1520-0493 doi: <https://doi.org/10.1175/MWR-D-18-0413.1> Available at <https://centaur.reading.ac.uk/89721/>

It is advisable to refer to the publisher's version if you intend to cite from the work. See [Guidance on citing](#).

To link to this article DOI: <http://dx.doi.org/10.1175/MWR-D-18-0413.1>

Publisher: American Meteorological Society

All outputs in CentAUR are protected by Intellectual Property Rights law, including copyright law. Copyright and IPR is retained by the creators or other copyright holders. Terms and conditions for use of this material are defined in the [End User Agreement](#).

www.reading.ac.uk/centaur

CentAUR

Central Archive at the University of Reading

Reading's research outputs online

1 **The Role of Local Orography on the Development of a Severe Rainfall Event**
2 **over Western Peninsular Malaysia: A case study.**

3 Mohd Fadzil Firdzaus Mohd Nor *

4 *Institute of Ocean and Earth Sciences, University of Malaya, Kuala Lumpur, Malaysia*

5 Christopher E. Holloway and Peter M. Inness

6 *Department of Meteorology, University of Reading, Reading, United Kingdom*

7 **Corresponding author address:* Mohd Fadzil Firdzaus Mohd Nor, Institute of Ocean and Earth
8 Sciences, University of Malaya, 50603 Kuala Lumpur, Malaysia.

9 E-mail: fadzil.mnor@um.edu.my

ABSTRACT

10 Severe rainfall events are common in western Peninsular Malaysia. They
11 are usually short and intense, and occasionally cause flash floods and land-
12 slides. Forecasting these local events is difficult and understanding the mech-
13 anisms of the rainfall events is vital for the advancement of tropical weather
14 forecasting. This study investigates the mechanisms responsible for a local
15 heavy rainfall event on 2 May 2012 that caused flash floods and landslides
16 using both observations and simulations with the limited-area high-resolution
17 UK Met Office Unified Model (MetUM). Results suggest that previous day
18 rainfalls over Peninsular Malaysia and Sumatra Island influenced the devel-
19 opment of overnight rainfall over the Strait of Malacca by low-level flow con-
20 vergence. Afternoon convection over the Titiwangsa mountains over Peninsu-
21 lar Malaysia then induced rainfall development and the combination of these
22 two events influenced the development of severe convective storm over west-
23 ern Peninsular Malaysia. Additionally, anomalously strong low-level north-
24 westerlies also contributed to this event. Sensitivity studies were carried out
25 to investigate the influence of the local orography on this event. Flattened
26 Peninsular Malaysia orography causes a lack of rainfall over the central part
27 of Peninsular Malaysia and Sumatra Island and produces a weaker overnight
28 rainfall over the Strait of Malacca. By removing Sumatra Island in the final
29 experiment, the western and inland parts of Peninsular Malaysia would re-
30 ceive more rainfall, as this region is more influenced by the westerly wind
31 from the Indian Ocean. These results suggest the importance of the interac-
32 tion between land masses, orography, low-level flow and the diurnal cycle on
33 the development of heavy rainfall events.

34 **1. Introduction**

35 Western Peninsular Malaysia is the most densely populated area of Peninsular Malaysia with at
36 least 65% of the Malaysian population. The Strait of Malacca is adjacent to the western coast of
37 Peninsular Malaysia and the eastern coast of Sumatra Island and is one of the busiest sea traffic
38 lanes in the world. This area has interesting weather patterns mostly affected by the interaction
39 between the atmosphere and local orography (Figure 1). In Peninsular Malaysia, severe weather
40 events such as flash floods, landslides, and strong wind storms are the main meteorological threats
41 affecting the socioeconomic factors of the people in this region. A better understanding of the
42 processes affecting such events is essential for improving forecasts and minimizing loss.

43 Localized convective rainstorms usually develop from thermal convection aided by warm sur-
44 face temperature and surface land heating due to solar insolation. Local orography, local weather
45 circulations such as land-sea breezes, and large-scale weather patterns such as monsoons will influ-
46 ence and modify local weather. For cases in Peninsular Malaysia and nearby islands, the following
47 mechanisms involved in the development of localized severe convection have been discussed in
48 previous studies:

- 49 1) the interaction between the gravity waves produced by the orography and the gravity waves
50 produced by the advancing westerly sea breeze front over the west coast (Joseph et al. 2008);
- 51 2) the daytime sea breeze being reinforced by the valley breeze circulation, enhancing convergence
52 over the mountainous region (Qian 2008);
- 53 3) the sea breeze collision between easterly and westerly sea breeze fronts enhancing convection
54 inland (Joseph et al. 2008; Qian 2008);
- 55 4) the interaction between the lee waves over the mountainous area and the westerly sea breeze
56 front which is common over northwest Peninsular Malaysia (Sow et al. 2011);

57 5) the gap wind associated with a strong wind from the east passing through the mountains push-
58 ing the inland convection toward the west (Sow et al. 2011).

59 These studies show the critical role of local orography and coastal circulations in developing and
60 modifying the weather in this region.

61 Fujita et al. (2010) argue that colder and denser low-level air flow ("cold flow", as compared
62 to surrounding air temperature) originates from the inland region of both Sumatra and Peninsu-
63 lar Malaysia usually formed from previous evening rainfall, is essential for convective activity
64 over the Strait of Malacca. The study found that after evening rainfalls at approximately 19:00
65 Malaysian Standard Time (MST, +08 UTC), in both Sumatra and Peninsular Malaysia there were
66 cold flows from both regions flowing toward the Strait of Malacca with a speed of $5-6 \text{ m s}^{-1}$ and
67 converging in the middle of the strait at approximately 01:00 MST. The peak time of the maximum
68 rainfall recorded over the strait was 05:00 MST. Fujita et al. (2010) also revealed that the width of
69 the Strait of Malacca (approximately 360 km between the mountain peaks of Sumatra and Penin-
70 sular Malaysia) affected the timing and location of the rainfall over the strait. Furthermore, in their
71 model experiment, when the gap between Sumatra and Peninsular Malaysia was widened orthog-
72 onally by an increment of approximately 100 km, the average peak time of maximum rainfall in
73 the middle of the strait are varied. For the 100 km-wide experiment, it was around 07:00 MST and
74 for the 200 km-wide experiment, the peak time of maximum rainfall in the middle of the strait was
75 around 10:00 MST. The 300 km-wide experiment showed that the peak time was 13:00 MST. In
76 the wider strait experiments (200 and 300 km experiments), the two cold flows from both regions
77 did not manage to converge before the rainfall as it rained before the two cold flows merged and
78 weaker convection was observed. Therefore, a wider strait caused a later and weaker rainfall.

79 Simulating precipitation over the tropics is subject to significant errors in accuracy in term of
80 location and time and as such remains open to improvement. Parameterized convection schemes

81 used in coarse resolution models generally show unrealistic results, such as an overestimated rain-
82 fall area or rainfall events that occur too early in the day as compared to observations (e.g. Birch
83 et al. 2016). Higher resolution models improve the representation of orography and they generally
84 have better mesoscale circulation and rainfall simulation, most likely because the models simulate
85 convective rainfall explicitly (Birch et al. 2016). While precipitation processes are complicated,
86 the physical mechanisms involved can be well represented by explicit convection simulation. For
87 example, a study from Golding (1993) showed that the 3 km MetUM model was able to capture
88 topographically forced thunderstorm genesis and the internal structure of thunderstorms including
89 the trade level inversion and mid-level rotation. Gravity waves are also generally well represented
90 by higher resolution models as in the 4 km MetUM Unified Model run in Love et al. (2011)
91 which simulated convection propagation over the Sumatra region. This study found that gravity
92 waves triggered offshore convection in the explicit convection model, but the insensitivity of the
93 convective parameterization in the lower resolution 40 km model was unable to correctly trigger
94 convection as the gravity waves passed.

95 To investigate the development of heavy rainfall over western Peninsular Malaysia, a case study
96 on 2 May 2012 was selected in which the Klang Valley (circled in red in Figure 1) experienced
97 severe convective storms that caused flash floods. This event disrupted everyday activities and
98 damaged property. The maximum hourly rainfall rate was 22 mm hr^{-1} and a total of 53.2 mm of
99 rain was observed within 5 hours at one of the nearest stations (Figure 2a and b). The maximum
100 rainfall occurred at 16:00 MST, weakened an hour later, and stopped at 18:00 MST. The heaviest
101 rainfall occurred mostly over the central west coast of the peninsula.

102 This event occurred during the inter-monsoon period (April-May and September-October, for
103 Malaysia). During this period, the Inter-tropical Convergence Zone climatologically occurs near
104 the equatorial region and increases local convective activity. The inter-monsoon period is also the

105 time when western Peninsular Malaysia receives a higher total of rainfall, especially from after-
106 noon rainfall, compared to the other seasons (MetMalaysia 2016). This is also shown in Figure 2c,
107 where climatological monthly mean of precipitation from Topical Rainfall Measurement Mission
108 (TRMM) is given for three regions of western and inland Peninsular Malaysia (red boxes in Figure
109 4). The total daily rain amount for this event in the west coast was 35.5 mm day^{-1} which is higher
110 than the 90th percentile of 20.3 mm day^{-1} (calculated by considering days averaging $\geq 1 \text{ mm}$
111 day^{-1}). Thus, this day is considered to be a heavy rainfall day. On 2 May 2012, Sumatra and
112 Peninsular Malaysia also experienced anomalously strong westerly winds from the Indian Ocean
113 and northwesterly winds over the Strait of Malacca (Figure 3). This event did not occur during a
114 Madden-Julian Oscillation (MJO) active phase; the Real-Time Multi-variate MJO index (Wheeler
115 and Hendon 2004) was less than 1 (weak MJO) between 25 April and 17 May 2012 (Bureau of
116 Meteorology Australia 2015). Additionally, the event also occurred during a neutral phase of El
117 Niño-Southern Oscillation (ENSO).

118 It was hypothesized that the evening rainfall over Peninsular Malaysia and Sumatra island on the
119 day before the event helped in generating rainfall over the Strait of Malacca overnight. Addition-
120 ally, the morning rainfall over the Strait of Malacca helped to induce the regeneration of convective
121 activity over the west coast of Peninsular Malaysia after merging with the rainfall cluster over the
122 Titiwangsa Mountains. Furthermore, stronger westerly and northwesterly winds from the Indian
123 Ocean helped enhance the development of the heavy convective rainfall. This study investigated
124 the mechanisms involved in the development of the rainfall event using the high-resolution Me-
125 tUM. While other studies have focused on modifying thermodynamic features (Fujita et al. 2010;
126 Sow et al. 2011) and moving land masses (Fujita et al. 2010) to study the convective rainfall mech-
127 anism in this specific region, this study will evaluate the importance of orography and land versus
128 sea regions on rainfall development by flattening mountains and removing the island of Sumatra.

129 **2. Data and Methodology**

130 *a. Data*

131 This study used the 3-hourly data from the Tropical Rainfall Mission Measurement (TRMM,
132 3B42 Version 7) which has $0.25^\circ \times 0.25^\circ$ resolution where all values are in mm hr^{-1} (Huffman
133 and Bolvin 2007). The 3B42 algorithm produces an adjusted rainfall rate which combines other
134 precipitation estimates from the TRMM Microwave Imager (TMI), Special Sensor Microwave
135 Imager (SSM/I), Advanced Microwave Scanning Radiometer for Earth Observing System (AMSR-
136 E), Special Sensor Microwave Imager/Sounder (SSMIS), Microwave Humidity Sounder (MHS),
137 Advanced Microwave Sounding Unit (AMSU), and microwave-adjusted merged geo-infrared (IR)
138 (Huffman and Bolvin 2007).

139 An hourly rainfall dataset of rain gauge measurements from Petaling Jaya station of the
140 Malaysian Meteorological Department (MetMalaysia) was used as a reference. Radar images
141 from the Malaysian Meteorological Department (MetMalaysia) from 00:00 MST 2 May 2012 -
142 20:00 MST 2 May 2012 were used to detect the location and time of the rainfall. According to
143 Kamaruzaman et al. (2012), MetMalaysia uses the Z-R relationship method of Marshall-Palmer
144 (Marshall and Palmer 1948; Battan 1973) to convert the reflectivity (Z , in $\text{mm}^{-6} \text{m}^3$) to rain rate
145 (R , in mm hr^{-1}) using the $Z=200R^{1.6}$ formula. At the time of this study conducted, MetMalaysia
146 used an optimization method (regression technique) to find the best correlation and minimize the
147 error between Z and R since there was no disdrometer instrument to measure raindrop size distri-
148 bution in Malaysia (Kamaruzaman et al. 2012).

149 Other data mentioned or used include the GES DISC Multi-year Monthly Mean Product from
150 AIRS Monthly Retrieval Data AIRX3STM_V006 which can be found on the Giovanni website
151 (NASA 2019) for surface air temperature anomalies, and the NCEP/NCAR Reanalysis Project

152 from the National Oceanic and Atmospheric Administration (NOAA) PSD, Boulder, Colorado,
153 USA, taken from their website for wind anomalies (NOAA 2019). The AIRS data were avail-
154 able from September 2009 until September 2016 at 1° spatial resolution. The data were Level 3
155 monthly gridded standard retrieval product using the AIRS infrared spectrometer, a visible imager,
156 and two microwave radiometers which were Advanced Microwave Sounding Unit (AMSU) with-
157 out the Humidity Sounder for Brazil (HSB). The NCEP/NCAR Reanalysis data was on a $2.5^\circ \times$
158 2.5° global grid, with 17 pressure levels.

159 *b. Model Setup*

160 The model setup in this study was similar to Holloway et al. (2013). A limited area model of
161 MetUM version 7.5 was used with two domains (see Figure 4), with a 12 km grid spacing for the
162 outer domain and a 1.5 km grid spacing for the inner domain. The model used the New Dynam-
163 ics dynamical core based on semi-implicit semi-Lagrangian and non-hydrostatic Euler equations
164 (Davies et al. 2005). The 12-km model (154×172 grid) used a $0.11^\circ \times 0.11^\circ$ resolution while
165 the 1.5-km model (666×814 grid) used a $0.0135^\circ \times 0.0135^\circ$ resolution. There were 38 vertical
166 levels in the 12-km model and 70 vertical levels in the 1.5-km model. The 12-km model had a
167 maximum height of 37 km, and the 1.5-km model had a maximum height of 40 km. The 12-km
168 model used a parameterized convection scheme and the lateral boundary conditions (LBCs) were
169 updated from ECMWF analyses every 6 hours, using a rim of 8 model grid points around the do-
170 main. The 1.5-km model lateral boundary condition were updated from the 12-km model output
171 every 30 minutes using an 8 model grid point rim width. The rim is the place at which the prog-
172 nostic fields were blended linearly between the outer analysis or driving model data and the inner
173 model domain. The model setup was one-way nested.

174 The model physics in the 12-km model used a modified Gregory-Rowntree convective param-
175 eterization with 30-min convective available potential energy (CAPE) relaxation time scale, thus
176 using CAPE as the basis of its closure (Gregory and Rowntree 1990). The 12-km model also used
177 a standard boundary layer scheme for vertical subgrid mixing (Lock et al. 2000) without hori-
178 zontal subgrid mixing. This model also used single-moment mixed-phase microphysics with two
179 components which are liquid water and ice/snow (Wilson and Ballard 1999). The model physics
180 in the 1.5 km model was the same as in the 4-km 3Dsmag model in Holloway et al. (2013) but
181 was reduced to a 1.5 km grid. The same CAPE-limited version of the convective parameteriza-
182 tion was used, and over 99% of the rainfall was generated explicitly (Lean et al. 2008). Based
183 on previous literature, convective parameterization in the 1.5 km model helped with the model's
184 stability, but the parameterization should not have had much of an effect on deep convection and
185 resulting circulations (Lean et al. 2008; Love et al. 2011; Holloway et al. 2012). The model used
186 the Smagorinsky-type subgrid mixing in all three dimensions. No boundary layer scheme (as in
187 the 12-km model) was used. The Smith cloud physics scheme (Smith 2014) was used in both
188 12-km and 1.5-km model simulations.

189 *c. Methodology*

190 Rainfall datasets from TRMM, gauges and radar images were used to detect the time and lo-
191 cation of the rainfall event. The control (CTR) run was used to compare the model output to the
192 observations and to analyze the development of this event in greater detail. Four sensitivity exper-
193 iments tested the role of local orography and land versus sea coverage in the development of the
194 event. The same model reconfiguration (to create the initial condition file) as in the CTR run was
195 used with the exception that the orography and land-sea mask fields were modified in an ancillary
196 file depending on the objective of the experiment. As the experiments were only run for the 1.5-km

197 model, all experiments used the same 12-km model LBC file as the CTR run. The experiments
198 were run on the same model period as in the CTR run. The modifications of each experiment are
199 represented in Figure 5.

200 The experiments modified the orography and land-sea mask as follows:

- 201 1. (**flatPM**) The orography of the peninsula and the closest small islands was flattened to sea
202 level.
- 203 2. (**flatSI**) The orography of Sumatra Island and the closest small islands was flattened to sea
204 level.
- 205 3. (**flatALL**) The orography of Peninsular Malaysia, Sumatra, and the surrounding small islands
206 was flattened to sea level.
- 207 4. (**noSI**) Sumatra was removed; the orography of Sumatra was initially flattened to sea level,
208 and the land-sea mask file was then adjusted by removing the land points (Sumatra and the
209 surrounding small islands) and replacing them with ocean points.

210 In the **noSI** experiment, the land point value in the land-sea mask file was changed to sea value
211 to represent the ocean and treated like an ocean. The roughness length and the surface latent heat
212 flux were considered the same as the ocean and the sea surface temperature was interpolated from
213 the nearest sea points.

214 To investigate the effects of orography modification on the rainfall amount, the peninsula was
215 divided into three regions - northwestern, western and inland peninsula as well as the central
216 strait (see Figure 4 in red) and the rainfall amounts for each region were calculated. This area
217 division was a modified version of the one used in Suhaila and Jemain (2009) which is based on
218 geographical division. The selection of the region over the strait (MS) was based on the majority of

219 rainfall that occurred in this case study. In all discussions hereafter, only 1.5-km model simulation
220 results are discussed.

221 **3. Results and Discussion**

222 *a. Observations*

223 Besides the information presented in the final part of the introduction section, the rainfall event
224 was also detected in radar images as shown in Figure 6 (top). A cluster of rainfall was observed
225 over the Strait of Malacca, as well as parts of northwestern and west-central Peninsular Malaysia
226 at 11:00 MST. By 12:00 MST, more rainfall clusters had spread across the western side of the
227 peninsula and along the Titiwangsa Mountains (see Figure 1) and became intense by 13:00 MST.
228 As the intensity of the rainfall increased over the western peninsula at 14:00 MST, the rainfall over
229 the Strait of Malacca weakened. The rainfall over the western peninsula strengthened and spread
230 to a larger area by 15:00 MST. It stayed on the west coast until 18:00 MST and had subsided at
231 20:00 MST (Figure 8a: C).

232 While it is common to have severe afternoon rainfalls during the intermonsoon period, observa-
233 tional data from the NASA's Atmospheric Infrared Sounder (AIRS) indicated that an anomalously
234 cold area of near-surface air had developed from Sumatra Island which had then propagated east-
235 ward into the Strait of Malacca from early April until early May 2012 (not shown). There was also
236 an anomalously strong westerly wind from the Indian Ocean and at the same time stronger north-
237 westerly wind over the northern part of the Strait of Malacca, on 1 and 2 May 2012 (Figure 3).
238 The Convective Available Potential Energy (CAPE) at the MetMalaysia's Sepang station revealed
239 that the CAPE value on the evening of 1 May (20:00 MST) was 2361 J kg^{-1} , and on the morning
240 of 2 May 08:00 MST was 1786 J kg^{-1} with the Convective Inhibition of -3.16 J kg^{-1} and -21.3 J

241 kg^{-1} respectively (University of Wyoming 2016). These conditions favored the development of a
242 severe rainstorm.

243 *b. Simulation : Control Run (CTR)*

244 The radar images (Figure 6a) showed the development of convective precipitation over western
245 Peninsular Malaysia at approximately 13:00 MST which intensified by 14:00 MST and 15:00
246 MST. As we have hypothesized earlier, the morning rainfall over the Strait of Malacca might
247 have helped to induce the development of convective activity over the west coast of Peninsular
248 Malaysia after merging with the rainfall cluster over the Titiwangsa Mountains. Although not
249 perfect in terms of location of the rainfall (Figure 6b), the model simulation reproduced most of
250 the rainfall event shown in the radar images. The main features, such as the rainfall over the strait
251 and along the Titiwangsa Mountains, are well represented. The model indicates more variability
252 in rainfall intensity over Peninsular Malaysia compared to the radar.

253 The 3-hourly mean precipitation from the TRMM (Figure 7) dataset demonstrates a realistic
254 comparison to the radar images (Figure 6a). Additionally, the TRMM dataset captured the rainfall
255 event in Peninsular Malaysia on the previous day (1 May) which was not available from the radar.
256 The model simulates the precipitation over the strait as in TRMM, although not perfectly. The
257 model also simulates other observed features such as rainfall events in the southeast (14:00 MST)
258 and the east coast of Peninsular Malaysia (17:00 MST).

259 The severe rainfall event in this simulation concentrated on the west coast at around 3°N to
260 4°N and the evolution of the rainfall event can be viewed in the time-longitude Hovmöller plot
261 in Figure 8a. On the day of the event (black horizontal dashed line), the rainfall over the strait
262 started around 05:00 MST on 2 May and propagated eastward within 9 hours for about 100
263 km or at approximately 3 m s^{-1} (Figure 8a: A). It mostly dissipated mostly before reaching the

264 coast. The rainfall over the Titiwangsa Mountains (Figure 8a: B) started around 12:00 MST and
265 within one hour propagated westward and eastward within one hour. Compared to TRMM in
266 Figure 8b, there were rainfall events over both landmasses before the event, agreeing with the
267 model (Figure 8a: E and 8b: Z). TRMM showed that there were rainfall events over the strait,
268 but these did not propagate as seen in the model (Figure 8a: A and 8b: V). Similar events over
269 both sides of the peninsula were in agreement between the model and TRMM (Figure 8a: C
270 and D versus 8b: X and Y). The rainfall that developed over the Titiwangsa mountains was also
271 captured in the model, similar to the TRMM (Figure 8a: B and 8b: W). The modeled westward-
272 propagating rainfall cluster lasted longer and was weaker than the observed cluster (Figure 8a: C
273 versus 8b: X). The modeled westward-propagating rainfall cluster later combined with the rainfall
274 event over the coast at approximately 14:00 MST (Figure 8a: C) and remained over the west coast
275 for a couple of hours. The modeled eastward-propagating rainfall cluster gradually subsided after
276 almost 30 minutes. However, another rainfall cluster over the east coast (Figure 8a: D) developed
277 and propagated eastward following the mean westerly wind. This figure indicated the rainfall event
278 that occurred on the previous day in both Sumatra Island and Peninsular Malaysia (Figure 8a: E)
279 could be one of the main factors that have contributed to the development of the severe event on 2
280 May in the Strait of Malacca.

281 The modeled mean wind circulation over 3°N to 4°N is shown in Figure 9 at 233-meter model
282 (hybrid) level (which is 233 m for columns beginning at sea level). The colors represent wind
283 speed, and the vectors represent the wind direction. Most of the time, the wind was stronger
284 in the Strait of Malacca compared to the Indian Ocean (leftmost area) and the South China Sea
285 (rightmost area). In the morning before the event (before the black dashed line), the winds over
286 the Strait of Malacca were mostly northwesterly (Figure 9 A). The westerly winds were stronger
287 and progressed eastward across the peninsula during the event (Figure 9 B). The northwesterly

288 winds were stronger over the peninsula before the rainfall event, on both 1 and 2 May (Figure 9
289 C). Although there were not enough days for analysis to make a robust determination, stronger
290 northwesterly winds in the strait may have been one of the main factors in the development of the
291 heavy rainfall over the western peninsula. The winds converged near the coast of the peninsula
292 before the event (Figure 9 D) and the convergence could have been associated with the rainfall
293 event. Stronger westerly winds before the event could also be a sign of stronger convection over
294 the peninsula before the event occurred.

295 The diurnal cycle of land-sea breeze can also be seen in Figure 9. A stronger sea breeze oc-
296 curred on both sides of the peninsula during the daytime. On the west coast of the peninsula,
297 the sea breeze became stronger by 12:00 MST and moved further inland. On the east coast of
298 the peninsula, the sea breeze began near the coast and gradually became stronger, starting off the
299 coast and moving inland (Figure 9 E). Note that the sea breeze over the east coast of the peninsula
300 in Figure 9(E) was constrained and not progressing further inland. It could have been affected by
301 the severe rainfall event over the western peninsula and the stronger north-easterly winds coming
302 from the strait and western peninsula. The land breeze (at night) on both the west and east coasts
303 of the peninsula was weaker except in the early morning of 3 May.

304 *c. Possible Mechanisms*

305 Possible mechanisms leading to the event on 2 May can be hypothesized by examining the
306 radar and the model in Figure 6. As seen in Figure 10, rainfall events from the afternoon of
307 1 May (Figure 10a: A and B)) might have influenced the development of the rainfall over the
308 Strait of Malacca and saturated the land especially over the west coast of the peninsula to cause
309 flooding on the next day. The rain intensified by 10:00 MST (Figure 10b: C), with the incoming
310 northwesterly winds assisting the development of convection by increasing low level convergence

311 and the lifting of boundary layer parcels over the strait. In the early afternoon, convective activity
312 was also observed over the Titiwangsa Mountains (Figure 10c). Later, these two rainfall clusters
313 from the strait and Titiwangsa mountains merged over the western peninsula (red arrows in Figure
314 10c), influencing the development of convection over the central west of Peninsular Malaysia
315 (Figure 10d: D) and produced rainfall. The Titiwangsa mountains blocked the rainfall cluster, and
316 the rainfall cluster which remained on the west coast despite the incoming northwesterly wind.
317 The local orography also helped to shape the direction of the wind. The westerly winds from
318 the Indian Ocean were deflected towards the Strait of Malacca by Sumatra Island in the north,
319 and the Titiwangsa Mountains in Peninsular Malaysia which kept the wind in a northwesterly
320 direction until it changed to westerly at the southern Peninsular Malaysia. The northwesterly wind
321 also influenced the convection over the Titiwangsa mountains which developed early at noon and
322 moved or redeveloped on the east coast.

323 Near-surface temperature and specific humidity were used to investigate the possible contribu-
324 tion of the moisture from the previous-day rainfall to the development of the morning rainfall over
325 the Strait of Malacca (Figure 11). Figure 11a shows the movement of anomalously cold near-
326 surface temperature (blue shades) toward the strait. Both flows (density current along with land
327 breezes) from Sumatra and the peninsula started moving slowly toward the strait around 23:00
328 MST and merged at the center of the strait. The moisture from previous rainfall was also trans-
329 ported toward the strait as shown in Figure 11b (red arrows). Higher moisture propagated slowly
330 toward the strait from both land masses commenced at 21:00 MST and clustered at the center of
331 the strait early on the morning of 2 May. Thus, the combination of colder air and moist air flows
332 from both land masses favored the development of convective rainfall over the Strait of Malacca by
333 providing additional moisture and low-level lift to the atmosphere. The converging flows can also
334 be viewed in Figure 12. By 04:00 MST, there was a sign of converging wind flowing toward the

335 center of the strait. The converging winds were more pronounced where the flows from the land
336 masses met the northwesterly wind flowing through the strait. This can also be cold outflow fronts
337 moving from the coast regions of the land masses toward the center of the strait. The converging
338 winds are co-located with, and plausibly contribute to the development of, scattered rainfall over
339 the strait (dashed contours in Figure 12) as early as 05:00 MST. Converging winds continued to
340 intensify through 08:00 MST and the rainfall clusters over the strait grew larger.

341 Sensitivity experiments were done to investigate how the local orography and Sumatra Island
342 affected the rainfall development in this event, and these will be discussed in the next section.

343 *d. The Role of Local Orography and Sumatra Island*

344 1) THE ROLE OF THE TITIWANGSA MOUNTAINS

345 As we have discussed earlier, the **flatPM** experiment was conducted to investigate the role of the
346 Titiwangsa Mountains (as in Figure 5, **flatPM**) and the result is shown in Figure 13e-h. The first
347 noticeable difference is the lack of organized convection inland of the peninsula on the afternoon of
348 1 May (Figure 13e: A). A rainstorm cluster was observed in the morning of 2 May over the Strait
349 of Malacca. The rainfall cluster over the Strait of Malacca was slightly tilted toward Peninsular
350 Malaysia (Figure 13f: B), and it is associated with the westerly and northwesterly winds from the
351 Indian Ocean. Without the Titiwangsa Mountains, these onshore winds are not restricted and are
352 able to progress further inland onto the peninsula, causing the northern part of the rainfall cluster
353 at the strait to be pushed toward the peninsula. Another difference is that in the early afternoon
354 of 2 May (Figure 13g: C) there was no convection inland of the peninsula. However, there was
355 still rainfall over the coast, due to the sea breeze interaction with the landmass. The event was less
356 intense than in the control, and later that day the convection was pushed to the southeast by the
357 prevailing northwesterly wind.

358 The Hovmöller Figure 14c shows the temporal evolution of rainfall clusters in the **flatPM** ex-
359 periment. The rainfall over the western peninsula was weaker as seen in Figure 14c (A) and over
360 time propagating eastward. The northwesterly wind influenced the rainfall cluster to propagate
361 eastward and this is also the reason for the lower amount of rainfall on the west coast of Penin-
362 sular Malaysia as most of the rainfall cluster was pushed eastward (Figure 14d). The Hovmöller
363 plot in Figure 14d shows the northwesterly winds observed over the Strait of Malacca the day
364 before and in the early morning before the event. The low-level winds were mostly westerly on
365 the afternoon of the event, and later the westerly wind advanced further inland (Figure 14d: B).
366 Compared to the control, the daytime wind was weaker (blue shades) and the nighttime wind was
367 stronger in the western peninsula when Titiwangsa mountains were removed. The northwesterly
368 wind was slightly weaker in the strait before (Figure 14d: C) and slightly stronger during the day
369 of the event (Figure 14d: B).

370 A weak easterly sea breeze observed on the east coast was associated with a weaker land-sea
371 temperature gradient (reducing the land-sea breeze strength) as well as the absence of orographic
372 convection inland of the peninsula. The plot in Figure 14d also shows some important wind-
373 rainfall relationships in this experiment. For example, rainfall over the Strait of Malacca is associ-
374 ated with the converging low-level winds near the west coast of the peninsula.

375 2) THE ROLE OF THE BARISAN MOUNTAINS

376 The **flatSI** experiment was conducted to look at the role of the Barisan Mountains in Sumatra,
377 and the result is shown in Figure 13i-1. In the late afternoon of 1 May (Figure 13i), there were
378 rainfall events in both Peninsular Malaysia and Sumatra although there was weaker rainfall in
379 Sumatra (Figure 13i: A). These rainstorms influenced the development of the rainfall event over
380 the Strait of Malacca on the morning of 2 May (Figure 13j: B). Orographic convective rainfall was

381 also observed over the peninsula (Figure 13k: C). The rainfall that developed over the west coast
382 of the peninsula was a combination of moist downdraft flow from the rainfall event over the Strait
383 of Malacca and the developing sea breeze near the coast which merged with the orographic rain-
384 fall over the peninsula. The Titiwangsa Mountains had blocked the rainfall cluster from moving
385 eastward for a couple of hours despite the prevailing northwesterly wind (Figure 13l).

386 The rainfall evolution in the **flatSI** experiment is shown as a Hovmöller plot in Figure 14e.
387 The Hovmöller figure revealed that rainfall over the west coast of the peninsula occurred slightly
388 earlier offshore than in the control run (around 1150 LT, Figure 14e: D) and propagated inland.
389 The rainfall mechanism on the peninsula is the same as the one in the control run. Unlike the
390 control run, there was less rainfall over Sumatra the day before, and rainfall from Sumatra started
391 from the east coast and propagated eastward toward the strait (Figure 14e: E).

392 The Hovmöller plot of the lower level wind (Figure 14f) shows that the absence of the Barisan
393 Mountains in Sumatra allows the westerly wind from the Indian Ocean to advance inland (Figure
394 14f: F). The wind over the strait on 1 May and early 2 May is weaker than in the control run. The
395 wind over the strait (near to the west coast of the peninsula) was northerly before and during the
396 event. The absence of Sumatra Island means there is no longer a narrow valley in between the
397 island and the peninsula and could be the reason for the weaker wind over the strait (Figure 14f:
398 G). On both days, the sea breeze over the east coast of Sumatra was generally weak.

399 3) THE ROLE OF BOTH THE TITIWANGSA AND BARISAN MOUNTAINS

400 The **flatALL** experiment investigates the effect of high altitude orography on the rainfall pattern
401 over the region. The flat landmasses caused weaker inland rainfall on 1 May (Figure 13m: A).
402 These rainfall events (1 May afternoon) were, however, still influencing the development of the
403 rainfall over the Strait of Malacca (Figure 13n). However, the rainfall cluster over the strait was

404 concentrated in the center of the strait, unlike in the control run. No orographic convective rainfall
405 is present over the peninsula and Sumatra (Figure 13o). However, the rainfall over the strait
406 still influenced the rainfall development on the northern part of the peninsula, and there was still
407 rainfall occurring over the west coast in the afternoon (Figure 13p), mostly due to the interaction
408 between the westerly wind, sea breeze and surface friction. Rainfall events were observed across
409 the western coast at approximately 15:00 MST and dissipated as they move eastward following
410 the northwesterly wind (not shown).

411 The rainfall evolution shown in Figure 14g indicated less rainfall on 1 May (Figure 14g: H),
412 more rainfall over the strait as the rainfall becomes concentrated in the center of the strait (Figure
413 14g: K), and less rainfall during the day of the event (Figure 14g: L). The rainfall that developed
414 over the western coast dissipated early and did not propagate eastward to the east coast in contrast
415 with the other experiments. There was also a rainfall event over the west coast throughout the night
416 between 1 May and 2 May. In the Hovmöller plot of the low-level wind in Figure 14h, the absence
417 of the mountains in both Sumatra and the peninsula caused the westerly wind to advance inland.
418 The wind was also weakened over the strait (Figure 14h: M) due to the absence of a narrow valley
419 surrounded by mountains as explained in the previous section. The winds were mostly westerly
420 in the early morning before the event. Without the orography, the westerly wind advanced inland
421 smoothly across the peninsula (Figure 14h: N). The sea-breeze on the day of the event over the
422 peninsula was also weakened as the stronger westerlies dominated the area.

423 4) THE ROLE OF SUMATRA ISLAND

424 The role of Sumatra Island was examined by conducting the **noSI** experiment as shown in Figure
425 13q-t. Rainfall events occurred on the afternoon of the previous day (Figure 13q), mostly in the
426 north and south of the peninsula. A few rainfall events had developed off the western coast by

427 late morning, and there was also some rainfall over the northwestern peninsula (Figure 13s). The
428 lack of early morning rain over the ocean did not prevent the rainfall development over the west
429 coast on the afternoon of 2 May (Figure 13s). There were also rainfall events over the Titiwangsa
430 Mountains from the orographic convention which lead to heavy rainfall over western peninsula
431 later in the afternoon of 2 May (Figure 13t). The rainfall evolution in Figure 14i shows a few ocean
432 rainfall events and the rainfall over the peninsula on 2 May which occurred almost simultaneously
433 across the peninsula. There was also an early morning rainfall event over the west coast (around
434 0250 LT) which lasted for more than 4 hours, and another rainfall event later that day (around
435 19:00 MST). These three rainfall events contributed to a large amount of the total daily rainfall on
436 2 May. Thus, without Sumatra Island, rainfall would have been more frequent over the west coast
437 from the 1 May until 2 May.

438 The winds would have been consistently westerly in the absence of Sumatra Island (Figure
439 14j: P). Interestingly, the westerly wind near the strait before the event was also weaker than the
440 corresponding wind in control run near the western coast of peninsula (Figure 14j: Q). This shows
441 that the narrow valley created by the mountains of both Sumatra Island and Peninsular Malaysia
442 are essential in creating stronger winds over the Strait of Malacca. The wind on the east coast
443 and the South China Sea (103.5° E - eastward) prior to and a few hours after the event was also
444 stronger than in the control run. One possible reason for this is that, as the winds reach the southern
445 tip of the Titiwangsa mountains, they are deflected toward the South China Sea. Thus, because of
446 the open ocean on the west, the western Peninsula of Malaysia is exposed to the westerly wind
447 from the Indian Ocean. The specific humidity over central western Peninsular Malaysia in this
448 experiment is also higher and is at least 0.87 g kg^{-1} on average when compared to the control run
449 (not shown). Therefore, it is plausible that there is more moisture transported from the west and

450 that this westerly wind with extra humidity enhanced convective activity and rainfall over the west
451 of Peninsular Malaysia.

452 5) COMPARISON OF RAINFALL AMOUNT

453 The rainfall amount on the north-west, central west, inland and central Strait of Malacca regions
454 (NWC, WC, IL, and MS respectively) from these experiments can be viewed in Figure 15. The
455 total rainfall on 2 May (event day) in the CTR experiment shows a higher amount compared to the
456 **flatPM** experiment in all four regions. The differences illustrate the importance of the Titiwangsa
457 mountains in maintaining the rainfall cluster to the west. The rainfall total in the CTR run is higher
458 in the WC and IL regions in the **flatSI** experiment although not in the NWC region. In the **flatALL**
459 experiment, the NWC and WC received more rainfall than in CTR on 2 May, since more rainfall
460 occurred in the coastal area rather than inland, as is further shown by the lower rainfall total in IL
461 (compared to CTR). The total rainfall in the **NoSI** experiment was generally higher in all regions
462 as compared to CTR on the 2 May, with the same reasons discussed earlier.

463 Most of the rainfall in the central area of the Strait of Malacca occurred on 2 May (Figure 15d).
464 Larger rainfall amount in this region in the **flatALL** experiment can be explained by the inability of
465 the rainfall cluster to merged together due to the absence of mountains in both Sumatra Island and
466 Peninsular Malaysia. The mountains controlled the air circulation, flow and shape of the rainfall
467 to almost a squall-line shape in this case study. Without these mountains, rainfall would mostly
468 be concentrated in the center of the strait. In the **NoSI** experiment, the rainfall was concentrated
469 more on the land mass (peninsula) rather than the ocean as Sumatra Island was removed.

470 These experiments affected each region differently, but four common results were found:

471 1. removing the orography over Peninsular Malaysia reduced the rainfall in all three regions,

- 472 2. rainfall over the Strait of Malacca still occurred regardless of the height of the orography of
473 both Sumatra and the peninsula,
- 474 3. both of the high mountain ranges in Sumatra and Peninsular Malaysia created a narrow valley
475 that is responsible for creating a stronger wind over the Strait of Malacca, and
- 476 4. removing Sumatra Island caused more rainfall over the western peninsula. The higher total
477 rainfall in the **NoSI** experiment was also attributed to the frequent rainfall events on 2 May
478 which occurred during the early morning, mid-morning and evening.

479 **4. Conclusion**

480 This study investigated the role of orography in the development of a severe rainfall event in
481 the Klang Valley region, Peninsular Malaysia on 2 May 2012. During the day itself, there were
482 stronger westerly winds observed over the northern Strait of Malacca, with an anomalously cold
483 near-surface air over Sumatra Island that moved eastward in late April and early May 2012. A case
484 study was simulated using a limited-area setup of the high-resolution MetUM. The 1.5-km model
485 realistically represented the rainfall event but slightly underestimated its intensity and had minor
486 location errors. The 1.5-km model was able to represent the rainfall on 1 May over Peninsular
487 Malaysia and Sumatra Island and the rainfall over the Strait of Malacca on the morning of 2 May.
488 The model also reproduced the rainfall over the Titiwangsa Mountains of Peninsular Malaysia on
489 2 May.

490 Four sensitivity experiments were conducted to investigate the role of orography and land ver-
491 sus sea coverage on the development of the rainfall in this region. In the **flatPM** experiment,
492 Peninsular Malaysia received less rainfall on 2 May compared to the CTR, as the absence of the
493 Titiwangsa Mountains did not favor inland rainfall. Another reason for less rainfall in the western

494 peninsula was because the northwesterly wind had pushed the rainfall cluster eastward with no
495 mountains blocking it. On 1 May, the convection over the Strait of Malacca existed because of
496 the influence of rainfall on Sumatra Island and the small-scale rainfall over western Peninsular
497 Malaysia. However, the rainfall intensity over the Strait of Malacca was weaker than in the CTR.

498 The **flatSI** experiment caused the rainfall over Sumatra Island on 1 May to be reduced signifi-
499 cantly, but the rainfall over the peninsula was almost the same as in the CTR, including the rainfall
500 over the Titiwangsa Mountains. This caused the rainfall activity in the Strait of Malacca to be
501 less intense on the morning of 2 May. The combination of the rainfall event over the strait and
502 the rainfall event over the Titiwangsa Mountains enhanced the severe rainfall event over western
503 Peninsular Malaysia on 2 May. However, the rainfall was less than in the CTR over the west coast
504 and inland.

505 When the orography of Sumatra Island and Peninsular Malaysia was flattened (**flatALL**), the
506 mean total rainfall over the west coast on 2 May was higher than in the CTR. The mean total rain-
507 fall was less in the inland region than in the CTR because of the absence of orographic rainfall over
508 the Titiwangsa Mountains. Prolonged rain from 1 May to the 2 May during midnight contributed
509 to the higher total rainfall in this experiment.

510 The final experiment (**noSI**) investigated the role of Sumatra Island. The total daily rainfall
511 over the west coast of Peninsular Malaysia increased significantly. Rainfall along the west coast
512 occurred three times on 2 May. The rainfall over the west coast occurred as early as 03:00 MST
513 on 2 May and stopped after 10:00 MST. Then, another rainfall event occurred at 12:00 MST for
514 almost six hours. At 20:00 MST, another rainfall event occurred near and in the west coast. These
515 events contributed to the high total rainfall in the region. One of the reasons for the frequent
516 rainfalls was the high humidity that is plausible come from the Indian Ocean.

517 Analysing the control simulation and the other four experiments, the development of the rainfall
518 events on 1 and 2 May can be explained by the following processes as shown in Figure 16:

- 519 1. Peninsular Malaysia and Sumatra Island experienced rainfall on the evening of 1 May evening
520 (Figure 16a).
- 521 2. The outflows (density currents) from the previous afternoon's rainfall from Sumatra Island
522 and Peninsular Malaysia, along with land breezes enhanced by the anomalously cold air over
523 Sumatra merged into the Strait of Malacca, causing convergence and low-level lifting and
524 triggering the development of convection overnight (Figure 16b).
- 525 3. At the same time, a strong northwesterly wind (blue arrow, Figure 16c) from the Indian
526 Ocean brought more moisture and helped to enhance and maintain the convective activity in
527 the Strait of Malacca which then developed into a rainfall cluster on the morning of 2 May
528 that lasted until noon (Figure 16c).
- 529 4. By noon of 2 May, another rainfall cluster developed over the Titiwangsa Mountains (Figure
530 16d).
- 531 5. Outflow from the rainfall cluster over the Strait of Malacca, along with a sea breeze, induced
532 convection over the west coast of the peninsula (Figure 16d).
- 533 6. The outflow mentioned earlier coming from the west and the outflow from the rainfall over
534 the Titiwangsa Mountains range enhanced the convective activity over the western peninsula
535 (Figure 16d).
- 536 7. As the sea breeze circulation strengthened during the day, the rainfall over the strait weak-
537 ened, and convection over the western peninsula then intensified and produced rainfall (Figure
538 16e).

539 8. As the rainfall over the west coast increased, the rainfall over the Titiwangsa Mountains
540 spread to the west and east. The two rainfall clusters along the west coast merged (Figure
541 16e).

542 9. The rainfall cluster became stationary on the western peninsula as the Titiwangsa Mountains
543 blocked it from moving eastward despite the prevailing northwesterly wind (Figure 16e).

544 10. The rainfall cluster continued for a couple of hours and then dissipated.

545 Overall, both Peninsular Malaysia and the Island of Sumatra are essential in the development
546 of rainfall events over the strait, regardless of the height of the orography. As shown in this case
547 study, orography can play a vital role in enhancing the convection activity over western Peninsular
548 Malaysia. Sumatra Island also plays a crucial role in influencing the local weather of the peninsula.
549 The study has demonstrated that the island of Sumatra has prevented western Peninsular Malaysia
550 from being wetter thus potentially preventing more severe flooding and landslides.

551 *Acknowledgments.* The first author is funded by Majlis Amanah Rakyat (MARA) Malaysia, and
552 all authors would like to thank MARA, MetMalaysia (for observational data), NERC (for the UK
553 Met Office Unified Model), NERC staff at the University of Reading, the members of Tropical
554 Hour Met@Reading for input, Stephanie Johnson for the help with the modification of land-mask
555 file for the experiments, Andrew Turner and Geoffrey Wadge for the comments throughout the
556 research and on the thesis, and John Marshall for the comments on the thesis. This work used the
557 ARCHER UK National Supercomputing Service (<http://www.archer.ac.uk>).

558 **References**

559 Battan, L. J., 1973: *Radar Observation of the Atmosphere*. University of Chicago Press.

560 Birch, C. E., S. Webster, S. C. Peatman, D. J. Parker, A. J. Matthews, Y. Li, and M. E. E. Hassim,
561 2016: Scale interactions between the MJO and the western Maritime Continent. *Journal of*
562 *Climate*, **29** (7), 2471–2492, doi:10.1175/JCLI-D-15-0557.1.

563 Bureau of Meteorology Australia, 2015: Madden-Julian Oscillation (MJO) Index. URL [http://](http://www.bom.gov.au/climate/mjo/graphics/rmm.74toRealtime.txt)
564 www.bom.gov.au/climate/mjo/graphics/rmm.74toRealtime.txt.

565 Davies, T., M. J. P. Cullen, a. J. Malcolm, M. H. Mawson, a. Staniforth, a. a. White, and N. Wood,
566 2005: A new dynamical core for the Met Office’s global and regional modelling of the atmo-
567 sphere. *Quarterly Journal of the Royal Meteorological Society*, **131** (608), 1759–1782, doi:
568 10.1256/qj.04.101.

569 Fujita, M., F. Kimura, and M. Yoshizaki, 2010: Morning Precipitation Peak over the Strait of
570 Malacca under a Calm Condition. *Monthly Weather Review*, **138** (4), 1474–1486, doi:10.1175/
571 2009MWR3068.1.

572 Golding, B. W., 1993: A Numerical Investigation of Tropical Island Thunderstorms. *Monthly*
573 *Weather Review*, **121**, 1417.

574 Gregory, D., and P. Rowntree, 1990: A Mass Flux Convection Scheme with Representation of
575 Cloud Ensemble Characteristics and Stability-Dependent Closure. *Monthly Weather Review*,
576 **(118)**, 1483.

577 Holloway, C. E., S. J. Woolnough, and G. M. S. Lister, 2012: Precipitation distributions for explicit
578 versus parametrized convection in a large-domain high-resolution tropical case study. *Quarterly*
579 *Journal of the Royal Meteorological Society*, **138** (668), 1692–1708, doi:10.1002/qj.1903.

580 Holloway, C. E., S. J. Woolnough, and G. M. S. Lister, 2013: The Effects of Explicit versus Pa-
581 rameterized Convection on the MJO in a Large-Domain High-Resolution Tropical Case Study.

582 Part II: Processes Leading to Differences in MJO Development. *Journal of the Atmospheric*
583 *Sciences*, **72** (7), 2719–2743, doi:10.1175/JAS-D-14-0308.1.

584 Huffman, G. J., and D. T. Bolvin, 2007: Real-Time TRMM Multi-Satellite Precipitation Analysis
585 Data Set Documentation. *Laboratory for Atmospheres, NASA Goddard Space Flight Center and*
586 *Science Systems and Applications, Inc*, 26.

587 Joseph, B., B. C. Bhatt, T. Y. Koh, and S. Chen, 2008: Sea breeze simulation over the Malay
588 Peninsula in an intermonsoon period. *Journal of Geophysical Research*, **113**, D20 122, doi:
589 10.1029/2008JD010319.

590 Kamaruzaman, M., M. Adam, and S. Moten, 2012: Rainfall Estimation from Radar Data.
591 *Malaysian Meteorological Department Publication*, (6).

592 Lean, H. W., P. a. Clark, M. Dixon, N. M. Roberts, A. Fitch, R. Forbes, and C. Halliwell, 2008:
593 Characteristics of High-Resolution Versions of the Met Office Unified Model for Forecasting
594 Convection over the United Kingdom. *Monthly Weather Review*, **136**, 3408–3424, doi:10.1175/
595 2008MWR2332.1.

596 Lock, A. P., A. R. Brown, M. R. Bush, G. M. Martin, and R. Smith, 2000: A New Boundary
597 Layer Mixing Scheme . Part I : Scheme Description and Single-Column Model Tests. *Monthly*
598 *Weather Review*, 3187–3199.

599 Love, B. S., A. J. Matthews, and G. M. S. Lister, 2011: The Diurnal Cycle of Precipitation over the
600 Maritime Continent in a High-Resolution Atmospheric Model. *Quarterly Journal of the Royal*
601 *Meteorological Society*, **137** (657), 934–947, doi:10.1002/qj.809.

602 Marshall, J. S., and W. M. Palmer, 1948: The size distribution of raindrops. *Quarterly Journal of*
603 *the Royal Meteorological Society*, **76**, 16–36.

604 MetMalaysia, 2016: General Climate of Malaysia. URL www.met.gov.my/pendidikan/iklim/
605 iklimmalaysia, 1 pp.

606 NASA, 2019: GIOVANNI v 4.30. URL <https://giovanni.gsfc.nasa.gov/giovanni/>.

607 NOAA, 2019: Physical Science Division of Earth System Research Laboratory. URL [https://www.](https://www.esrl.noaa.gov/psd/cgi-bin/db_search/SearchMenus.pl)
608 [esrl.noaa.gov/psd/cgi-bin/db_search/SearchMenus.pl](https://www.esrl.noaa.gov/psd/cgi-bin/db_search/SearchMenus.pl).

609 Qian, J.-H., 2008: Why Precipitation Is Mostly Concentrated over Islands in the Maritime Conti-
610 nent. *Journal of the Atmospheric Sciences*, **65** (4), 1428–1441, doi:10.1175/2007JAS2422.1.

611 Smith, R. N. B., 2014: A scheme for predicting layer clouds and their water content in a general
612 circulation model. *Quarterly Journal of Royal Meteorological Society*, **128** (5), 400–405, doi:
613 10.1017/S0022215114000723.

614 Sow, K. S., L. Juneng, F. T. Tangang, A. G. Hussin, and M. Mahmud, 2011: Numerical simulation
615 of a severe late afternoon thunderstorm over Peninsular Malaysia. *Atmospheric Research*, **99** (2),
616 248–262, doi:10.1016/j.atmosres.2010.10.014.

617 Suhaila, J., and A. A. Jemain, 2009: Investigating the impacts of adjoining wet days on the dis-
618 tribution of daily rainfall amounts in Peninsular Malaysia. *Journal of Hydrology*, **368**, 17–25,
619 doi:10.1016/j.jhydrol.2009.01.022.

620 University of Wyoming, 2016: Atmospheric Soundings - Wyoming Weather Web - University of
621 Wyoming. URL weather.uwyo.edu/upperair/sounding.html.

622 Wheeler, M. C., and H. H. Hendon, 2004: An All-Season Real-Time Multivariate MJO Index: De-
623 velopment of an Index for Monitoring and Prediction. doi:10.1175/1520-0493(2004)132<1917:
624 AARMMI>2.0.CO;2.

⁶²⁵ Wilson, D. R., and S. P. Ballard, 1999: A Microphysically based precipitation scheme for the UK
⁶²⁶ Meteorological Office Unified Model. *Quarterly Journal of the Royal Meteorological Society*,
⁶²⁷ **125**, 1607–1636.

628 **LIST OF FIGURES**

629 **Fig. 1.** The location of Peninsular Malaysia and Sumatra. The red circle over the central west
630 coast of the Peninsular Malaysia is known as Klang Valley region. The Klang valley area
631 covers an area of approximately in between 2.6°N to 3.4°N and from the coast line of the
632 western peninsula to 102°E where the Titiwangsa mountains located. The shades represent
633 the orography height. 32

634 **Fig. 2.** Rainfall recorded by raingauge in Petaling Jaya station of Malaysian Meteorological Depart-
635 ment located shown in Figure 1 for (a) hourly (b) accumulated rainfall. (c) Monthly mean
636 of precipitation of 3 regions (shown in Figure 4) from TRMM dataset. The data range are
637 from 1998 to 2013. 33

638 **Fig. 3.** Wind speed (vectors) and wind speed anomaly (shaded) of NCEP/NCAR PSD Reanalysis
639 dataset on 2 May 2012. 34

640 **Fig. 4.** The domains for the simulation studies. The outer domain is used in the 12-km model
641 simulation. The inner domain is used in the 1.5-km model simulation. The 1.5-km model
642 domain is 0° - 9°N and 94°E - 105°E. The red dash and letters represent regions which were
643 defined to calculate rainfall amount in the control run to be compared to the experiments.
644 NWC: northwest, WC: west, IL: inland and MS: Strait of Malacca. The shades represent
645 the orography height. 35

646 **Fig. 5.** The four sensitivity experiments; Flat Peninsular Malaysia orography (**flatPM**), flat Suma-
647 tra Island orography (**flatSI**), flat both Peninsular Malaysia and Sumatra Island orography
648 (**flatALL**), and the Sumatra Island was removed (**noSI**). The shades here represent the orog-
649 raphy height in meters. 36

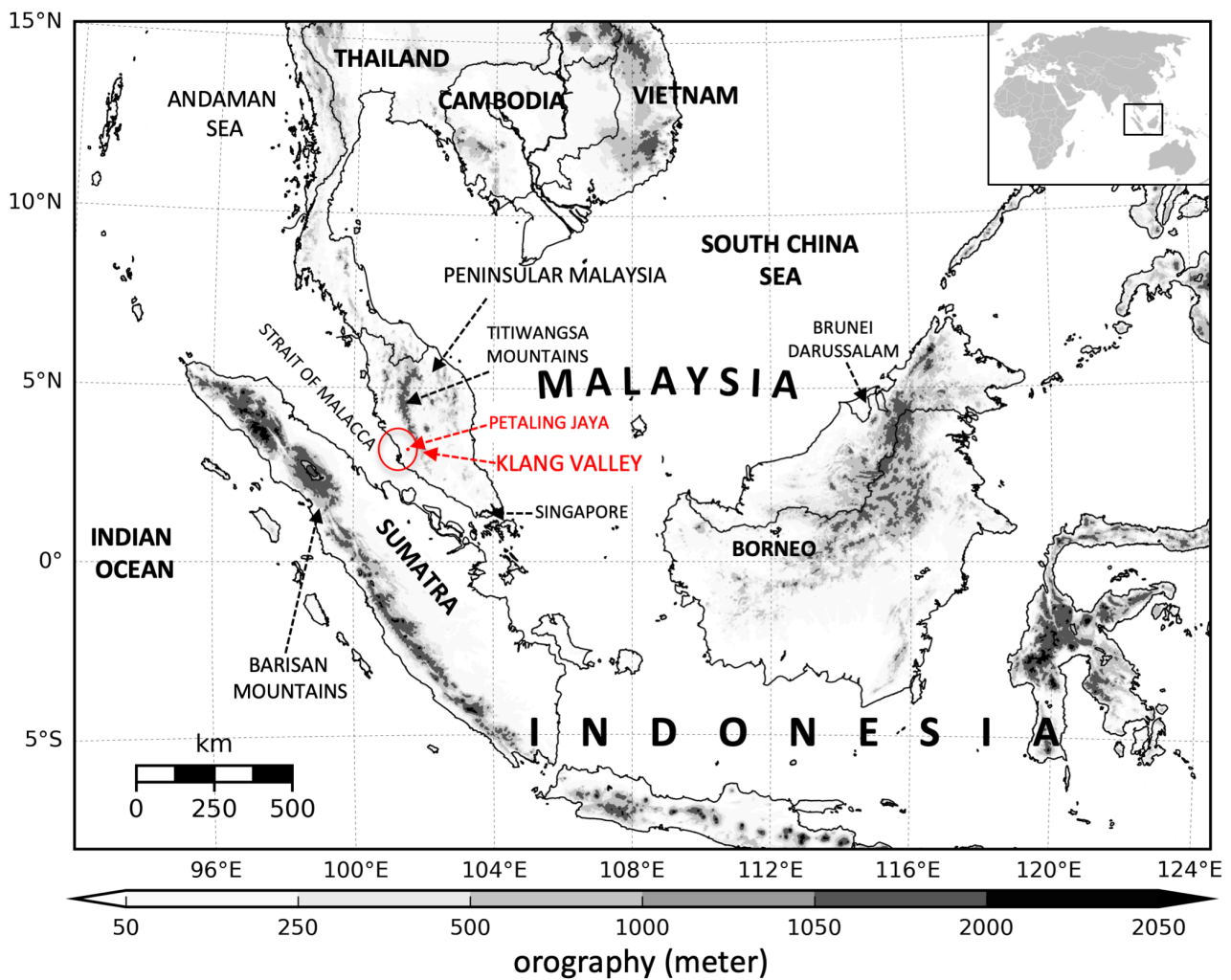
650 **Fig. 6.** Precipitation from radar (top) and 1.5-km model (bottom). Images are from 11:00 MST
651 of 2 May 2012 until 16:00 MST 2 May 2012. These times were selected to compare the
652 development of the rainfall event on 2 May in the afternoon. All values are in mm hr⁻¹.
653 Grey lines on land masses in bottom figures indicate orography feature of above 500 meters. 37

654 **Fig. 7.** The 3-hourly precipitation comparison between TRMM (top), and 1.5-km model (bottom).
655 The 3-hourly mean (as calculated in TRMM, but not at the same grid spacing) was compared
656 to the same rainfall scale, in mm hr⁻¹. Using TRMM, we are able to compare data on the
657 previous day between TRMM and model simulation. Black lines on land masses in bottom
658 figures indicate orography feature of above 500 meters. 37

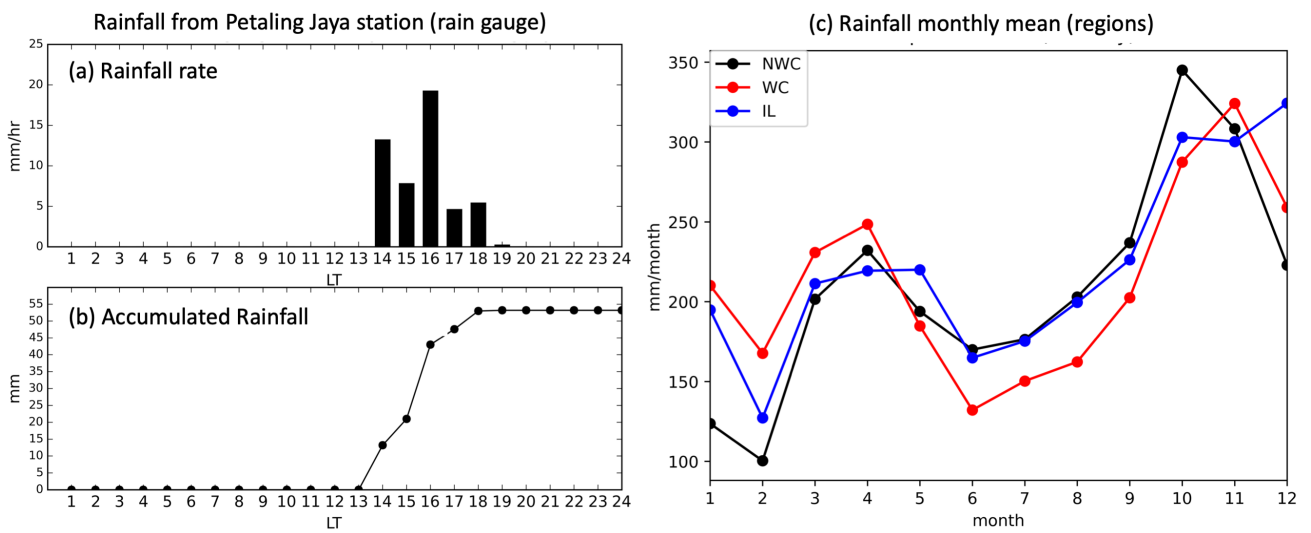
659 **Fig. 8.** (a)Time-longitude Hovmöller plot of precipitation from the 1.5-km model, averaged over
660 3°N to 4°N and, (b)Time-longitude Hovmöller plot of precipitation from TRMM dataset
661 averaged over 3°N to 4°N. The black dash line indicates the beginning time of the event.
662 The lines 96.7°E and 99.5°E represent the west and east coastlines of Sumatra Island re-
663 spectively. The lines 101.1°E and 103.5°E represent the west and east coastlines of the
664 Peninsular Malaysia respectively. The topography of both landmasses was also averaged
665 over 3°N to 4°N and shown at the bottom panel. The y-axis is time in Malaysian Standard
666 Time (MST). The x-axis is longitude. 38

667 **Fig. 9.** Same as in Figure 8 but for wind direction and magnitude (vectors) and speed (shades) from
668 the 1.5-km model at 233 m (hybrid model level). Black horizontal dashed line represent the
669 beginning time of the event. The contour line represents rainfall above 1 mm hr⁻¹. The
670 topography is shown at the bottom panel. The y-axis is time in Malaysian Standard Time
671 (MST). The x-axis is longitude. 39

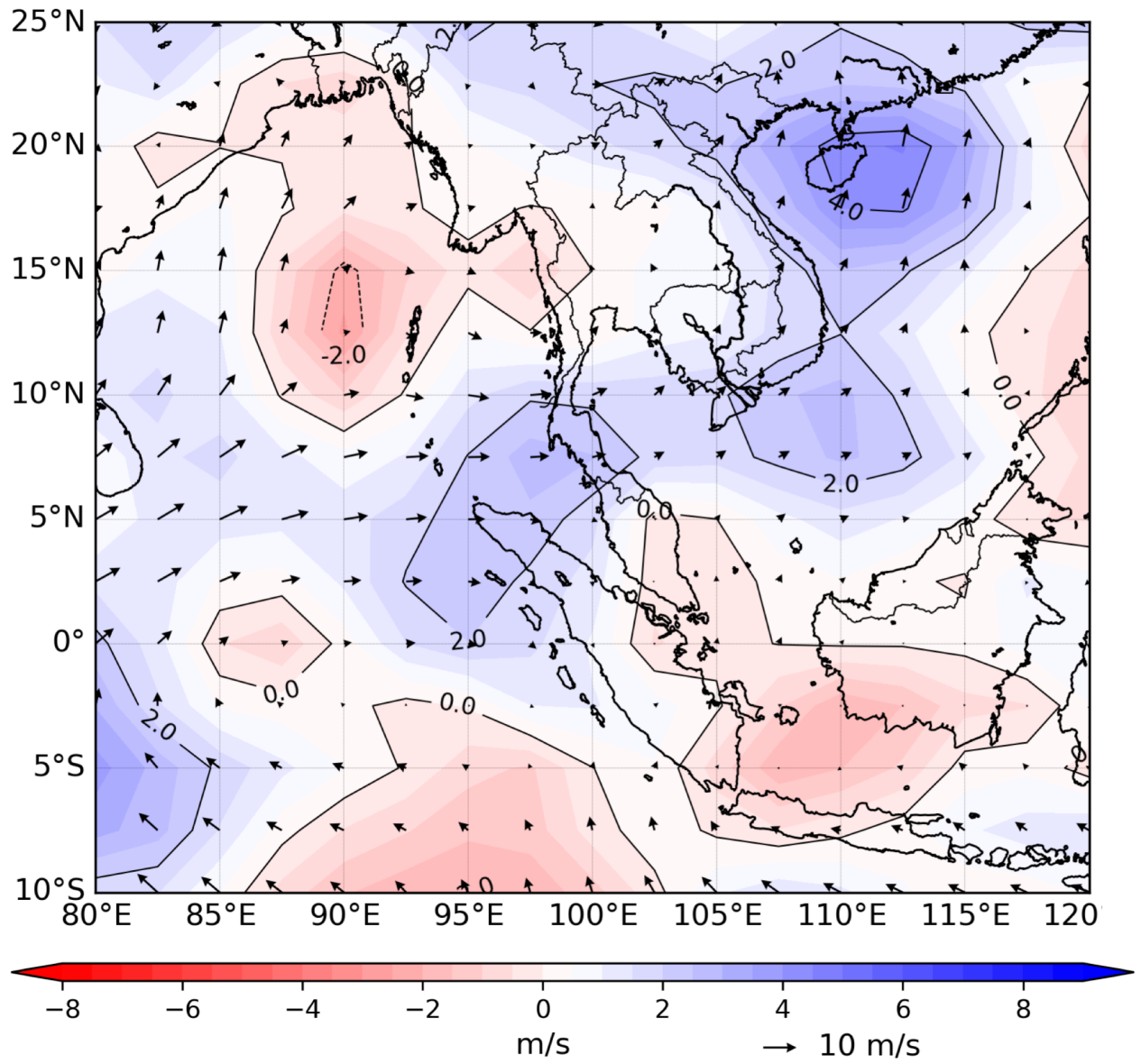
672	Fig. 10.	Precipitation and 850hPa winds from the 1.5-km model (CTR) showing the possible mechanisms for this event. (a) Afternoon rainfall on the 1 May (labeled A and B) provided extra moisture to the region to produce overnight rainfall over the Strait of Malacca as shown in panel (b). (c) Later, the convection over the strait and the rainfall in the mountains region over the peninsula influenced the development of rainfall events over the west coast as shown in panel (d). Grey lines on land masses indicate orography feature of above 500 meters.	40
678	Fig. 11.	Time-longitude Hovmöller plot, averaged over 3°N to 4°N, of (a) near-surface air temperature anomaly (21m hybrid level, shaded) and near-surface wind (13 m hybrid level, vectors) averaged over 3°N to 4°N from the 1.5-km model. The red arrows show cold outflows moving toward the center of Strait of Malacca. The temperature anomaly is the departure from 48-hour mean temperature. (b) near-surface specific humidity (21m hybrid level, shaded). Red arrows indicate the movement of humidity from both land masses toward the strait overnight. Black horizontal dashed lines represent the beginning time of the event. Dotted contour line indicated a 0 °C and 0 kg/kg values, respectively. The y-axis is time in Malaysian Standard Time (MST), 24-hour format. The x-axis is longitude.	41
687	Fig. 12.	Convergence/divergence plot in the morning of 2 May 2019 from the model simulation showing where the converging winds were likely to occur. Red-brown color represent converging winds and blue color represent diverging winds. Dashed black line represent rainfall above 1 mm hr ⁻¹ . Green arrows represent winds. All at 13.3 meter model level. Lower right figure shows the plot area.	42
692	Fig. 13.	Precipitation and 850hPa winds for comparison between control run, flat Peninsular Malaysia (flatPM), flat Sumatra (flatSI), flat Peninsular Malaysia and Sumatra (flatALL), and no Sumatra (noSI) experiments. The figure compares the main mechanisms in the development of the rainfall on 2 May, in Figure 10. Grey lines on land masses with no orography modification indicate orography feature of above 500 meters.	43
697	Fig. 14.	Same as in Figure 8a and 9 but for all of the experiments. (a,c,e,g,i) precipitation averaged over 3°N to 4°N. (b) 233 m wind (vectors) and wind speed (shaded) averaged over 3°N to 4°N. (d,f,h,j) Same as in (b) but colors represent the wind speed difference from the control run. The same color bar scale is used for both wind speed and wind speed difference. An additional contour line represents the rainfall above 1 mm hr ⁻¹ was added to the figure. Horizontal black dashed lines indicate the beginning of the event. Panel a and b are for reference only. The y-axis is time in Malaysian Standard Time (MST), 24-hour format. The x-axis is longitude.	44
705	Fig. 15.	Daily precipitation totals for the three regions of interest: (a) northwest coast, NWC, (b) west coast, WC and (c) inland, IL. (d) The central region of the Strait of Malacca, MS, and (e) the location of each region.	45
708	Fig. 16.	(left column) Key mechanisms involved in the development of the severe rainfall event over the west coast of Peninsular Malaysia starting from 1 May and on 2 May. The time is in local standard time and a close estimation of when the mechanisms start to occur. (right column) Key findings on the key mechanism in all experiments. (Illustrated by the first author.)	46



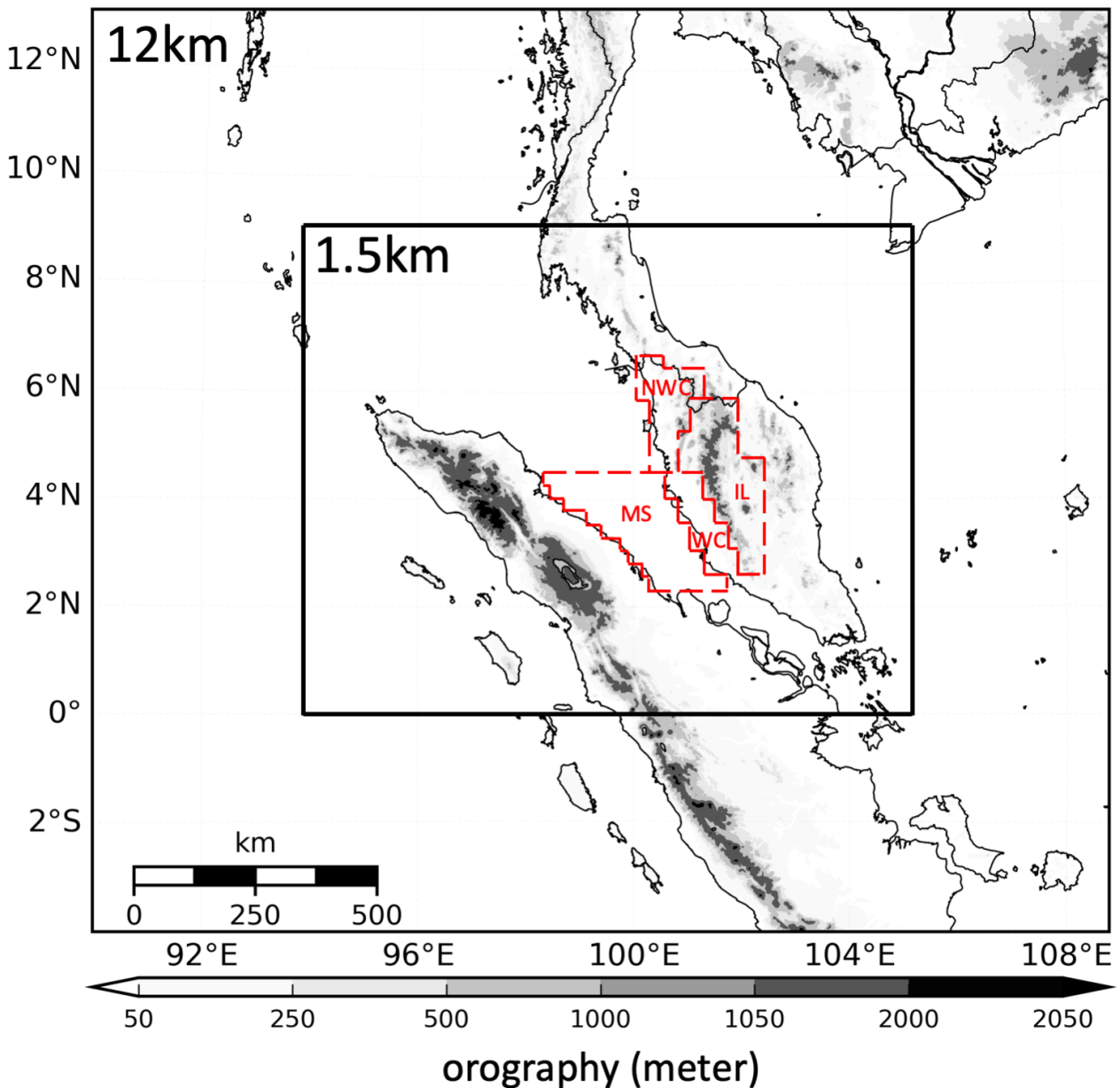
712 FIG. 1. The location of Peninsular Malaysia and Sumatra. The red circle over the central west coast of the
 713 Peninsular Malaysia is known as Klang Valley region. The Klang valley area covers an area of approximately
 714 in between 2.6°N to 3.4°N and from the coast line of the western peninsula to 102°E where the Titiwangsa
 715 mountains located. The shades represent the orography height.



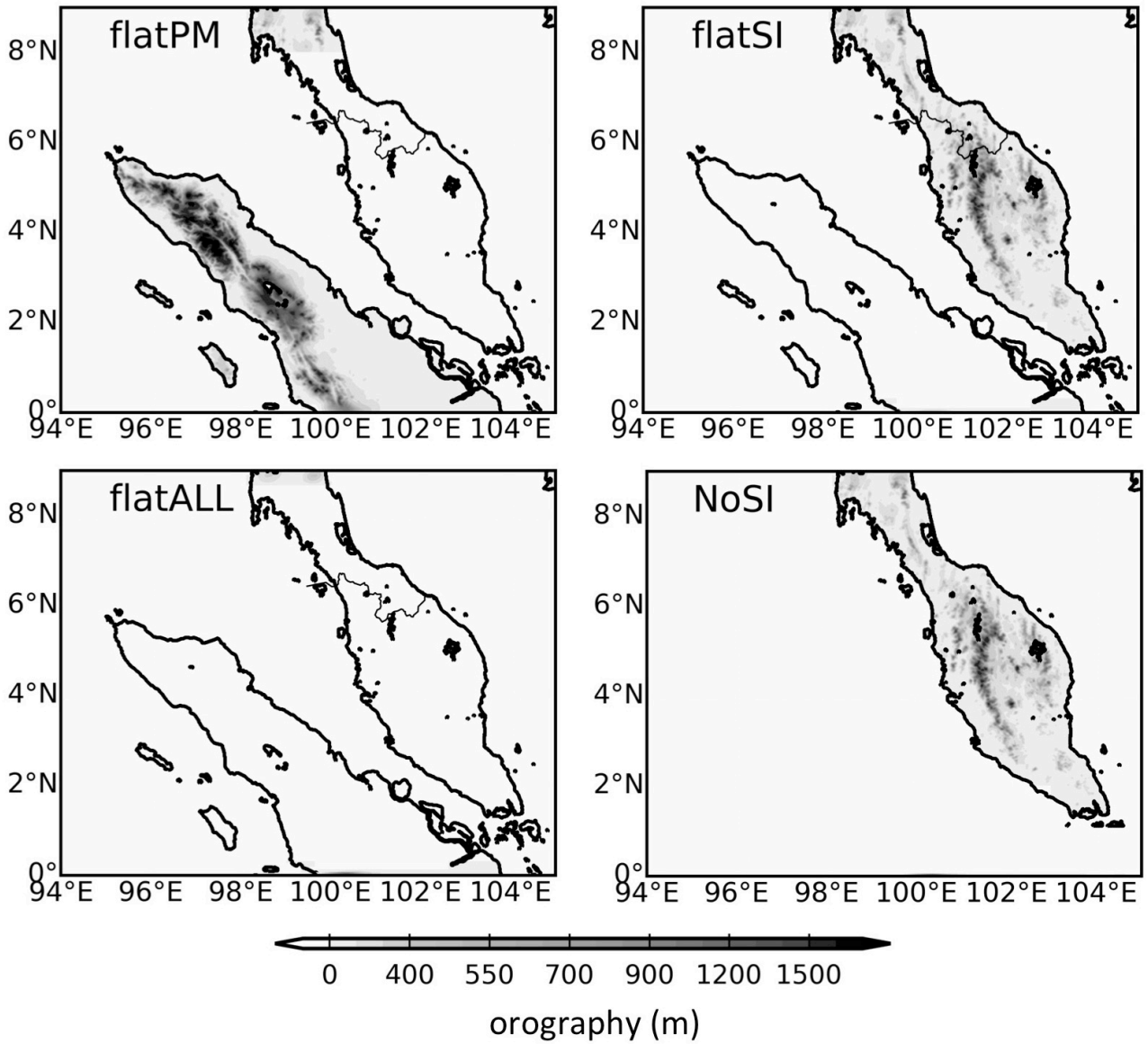
716 FIG. 2. Rainfall recorded by raingauge in Petaling Jaya station of Malaysian Meteorological Department
 717 located shown in Figure 1 for (a) hourly (b) accumulated rainfall. (c) Monthly mean of precipitation of 3 regions
 718 (shown in Figure 4) from TRMM dataset. The data range are from 1998 to 2013.



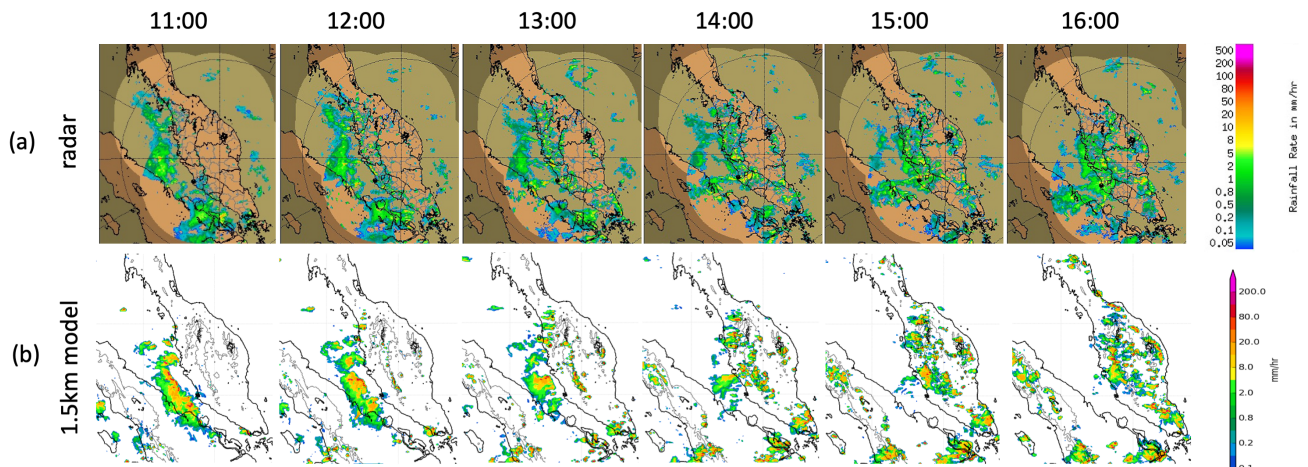
719 FIG. 3. Wind speed (vectors) and wind speed anomaly (shaded) of NCEP/NCAR PSD Reanalysis dataset on
 720 2 May 2012.



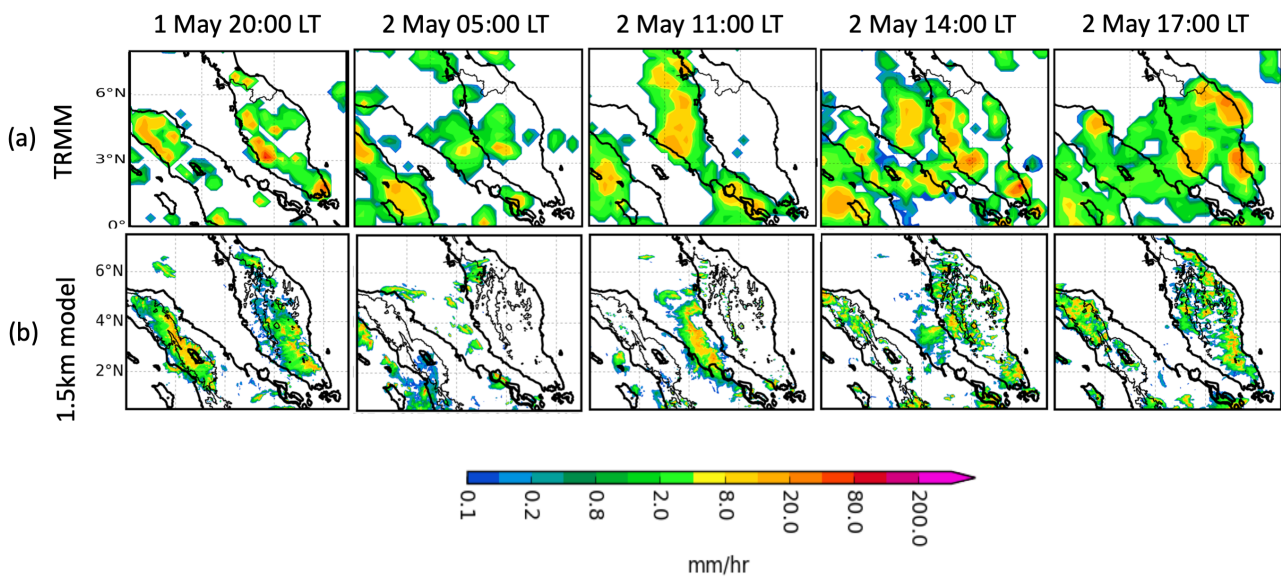
721 FIG. 4. The domains for the simulation studies. The outer domain is used in the 12-km model simulation.
 722 The inner domain is used in the 1.5-km model simulation. The 1.5-km model domain is 0° - 9°N and 94°E -
 723 105°E. The red dash and letters represent regions which were defined to calculate rainfall amount in the control
 724 run to be compared to the experiments. NWC: northwest, WC: west, IL: inland and MS: Strait of Malacca. The
 725 shades represent the orography height.



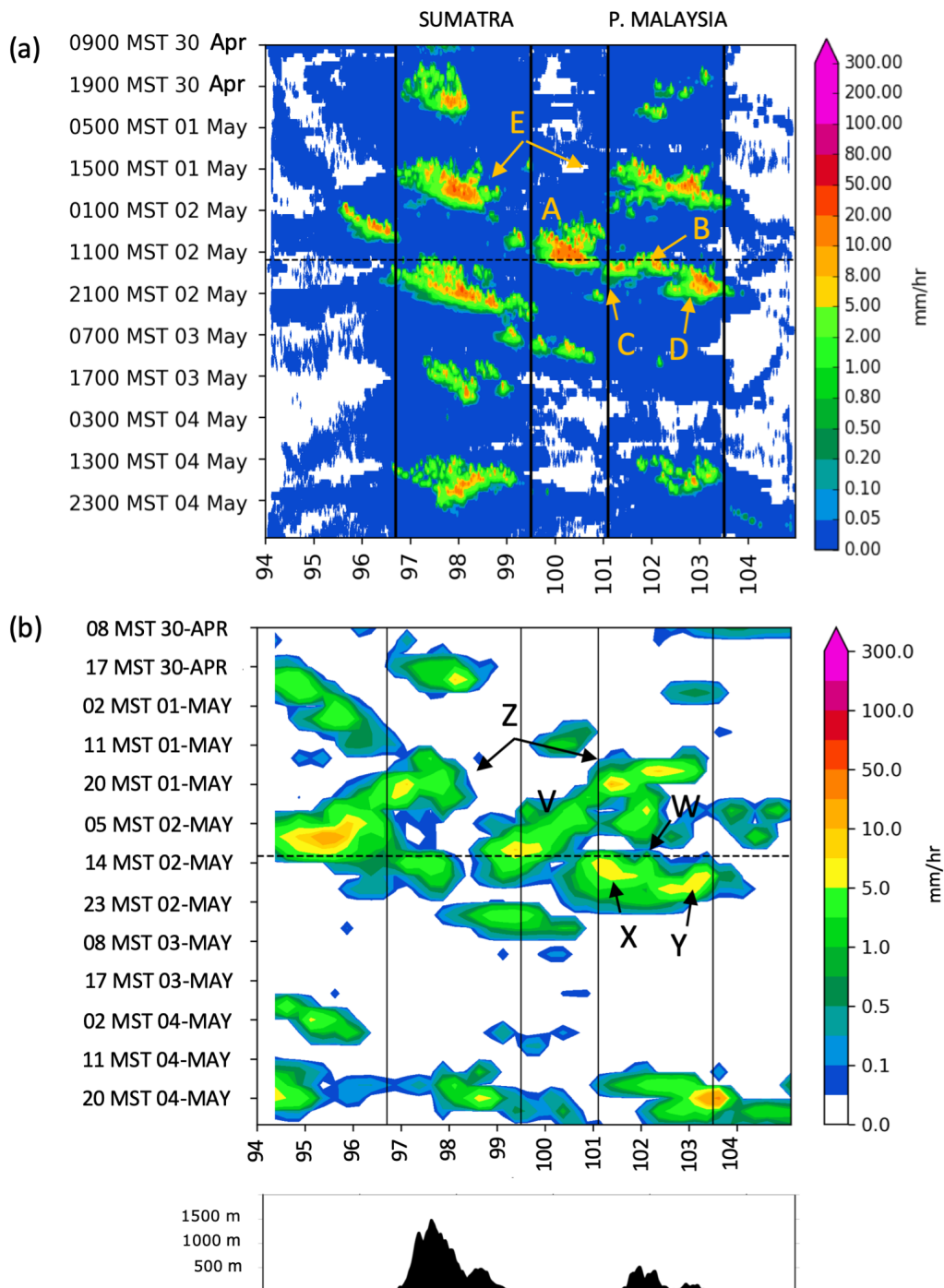
726 FIG. 5. The four sensitivity experiments; Flat Peninsular Malaysia orography (**flatPM**) , flat Sumatra Island
 727 orography (**flatSI**), flat both Peninsular Malaysia and Sumatra Island orography (**flatALL**), and the Sumatra
 728 Island was removed (**noSI**). The shades here represent the orography height in meters.



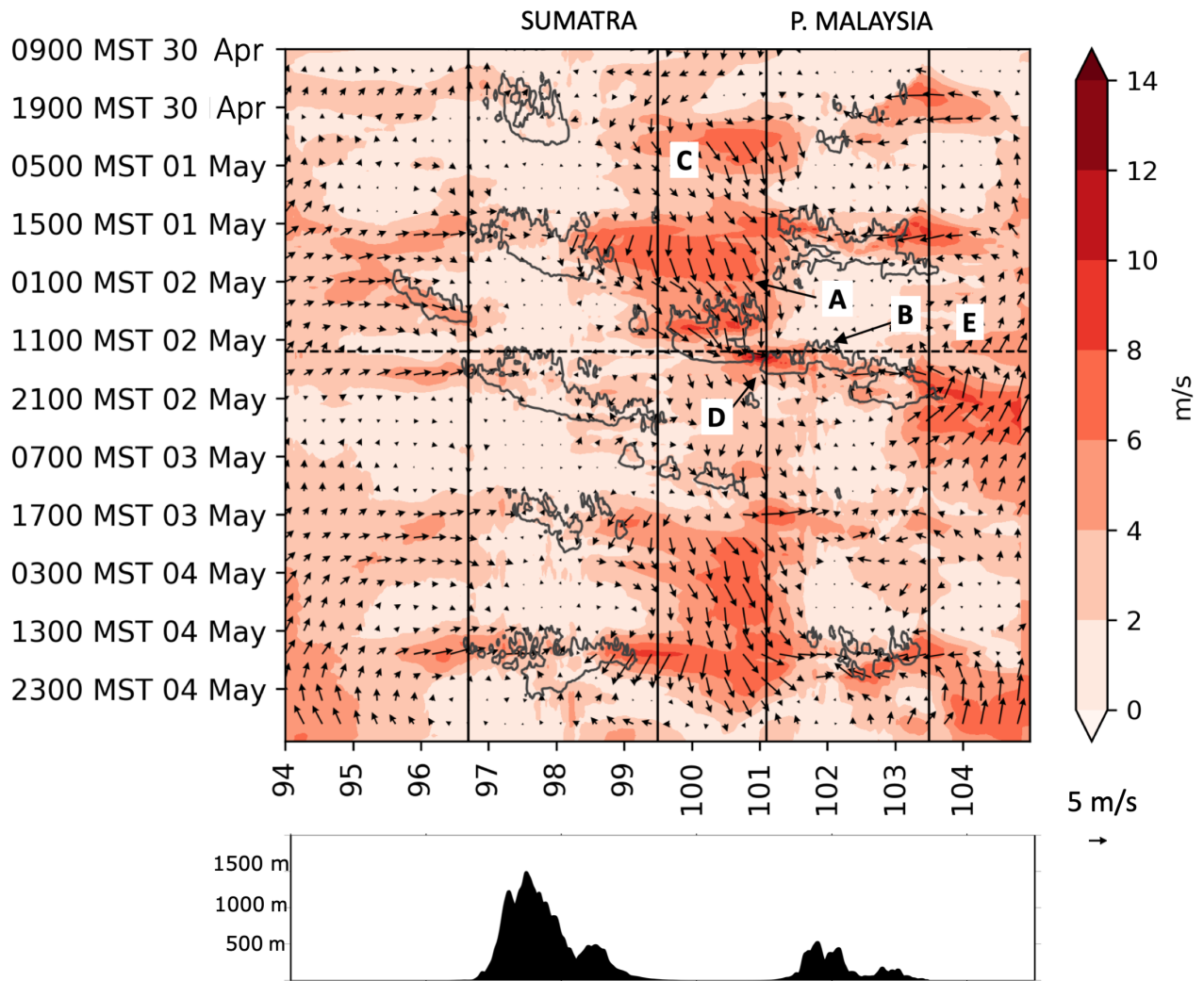
729 FIG. 6. Precipitation from radar (top) and 1.5-km model (bottom). Images are from 11:00 MST of 2 May
 730 2012 until 16:00 MST 2 May 2012. These times were selected to compare the development of the rainfall event
 731 on 2 May in the afternoon. All values are in mm hr^{-1} . Grey lines on land masses in bottom figures indicate
 732 orography feature of above 500 meters.



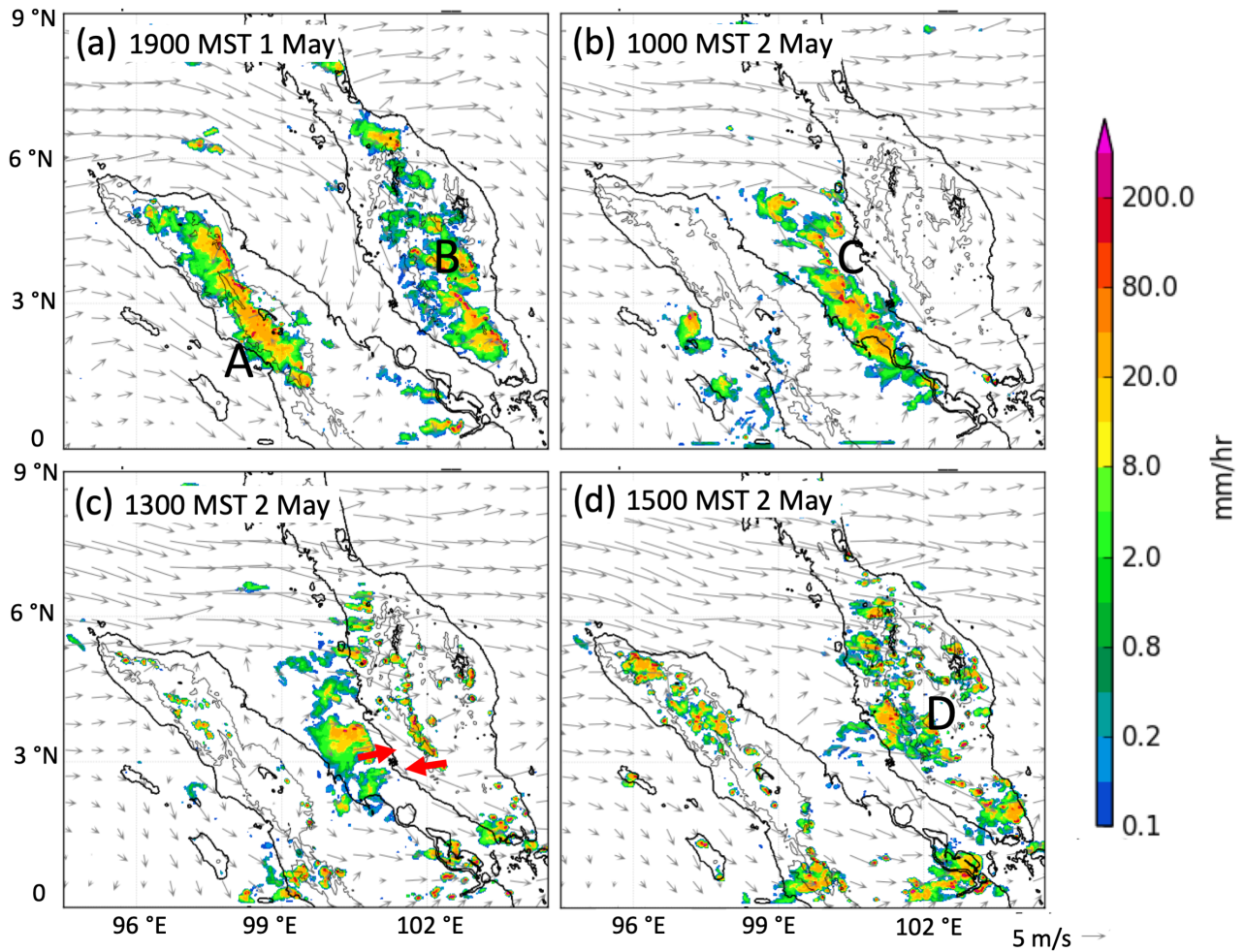
733 FIG. 7. The 3-hourly precipitation comparison between TRMM (top), and 1.5-km model (bottom). The 3-
 734 hourly mean (as calculated in TRMM, but not at the same grid spacing) was compared to the same rainfall
 735 scale, in mm hr^{-1} . Using TRMM, we are able to compare data on the previous day between TRMM and model
 736 simulation. Black lines on land masses in bottom figures indicate orography feature of above 500 meters.



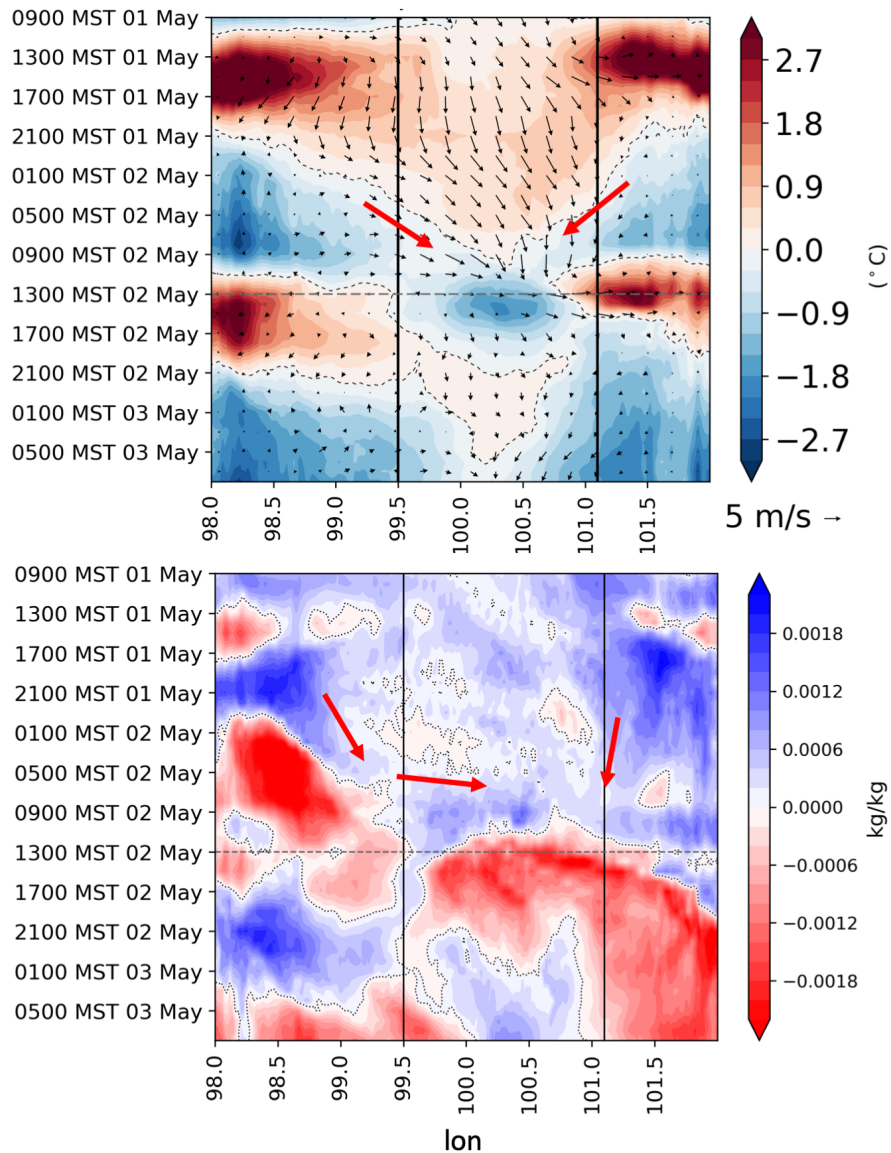
737 FIG. 8. (a)Time-longitude Hovmöller plot of precipitation from the 1.5-km model, averaged over 3°N to
 738 4°N and, (b)Time-longitude Hovmöller plot of precipitation from TRMM dataset averaged over 3°N to 4°N.
 739 The black dash line indicates the beginning time of the event. The lines 96.7°E and 99.5°E represent the west
 740 and east coastlines of Sumatra Island respectively. The lines 101.1°E and 103.5°E represent the west and east
 741 coastlines of the Peninsular Malaysia respectively. The topography of both landmasses was also averaged over
 742 3°N to 4°N and shown at the bottom panel. The y-axis is time in Malaysian Standard Time (MST). The x-axis
 743 is longitude.



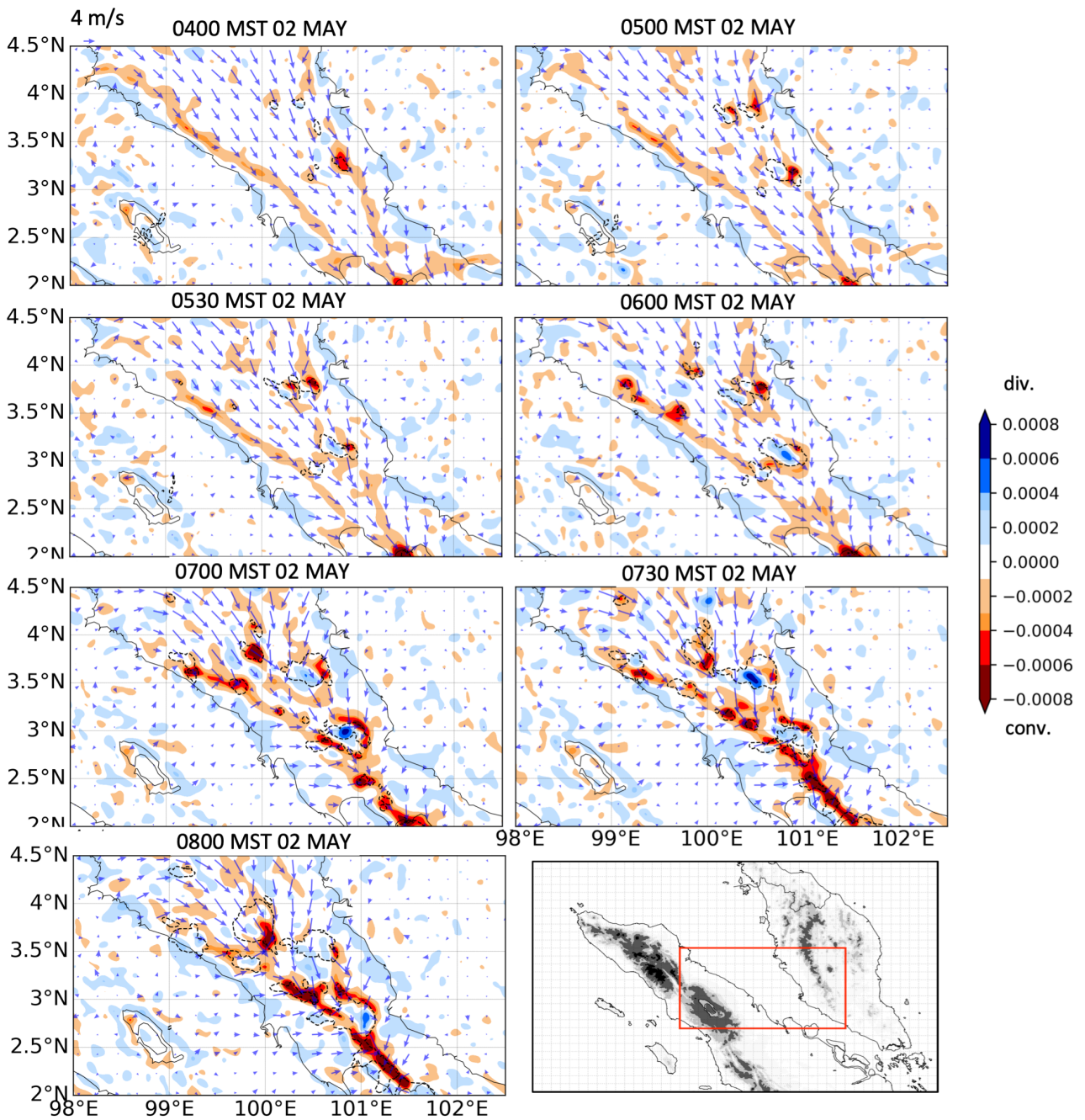
744 FIG. 9. Same as in Figure 8 but for wind direction and magnitude (vectors) and speed (shades) from the
 745 1.5-km model at 233 m (hybrid model level). Black horizontal dashed line represent the beginning time of the
 746 event. The contour line represents rainfall above 1 mm hr⁻¹. The topography is shown at the bottom panel. The
 747 y-axis is time in Malaysian Standard Time (MST). The x-axis is longitude.



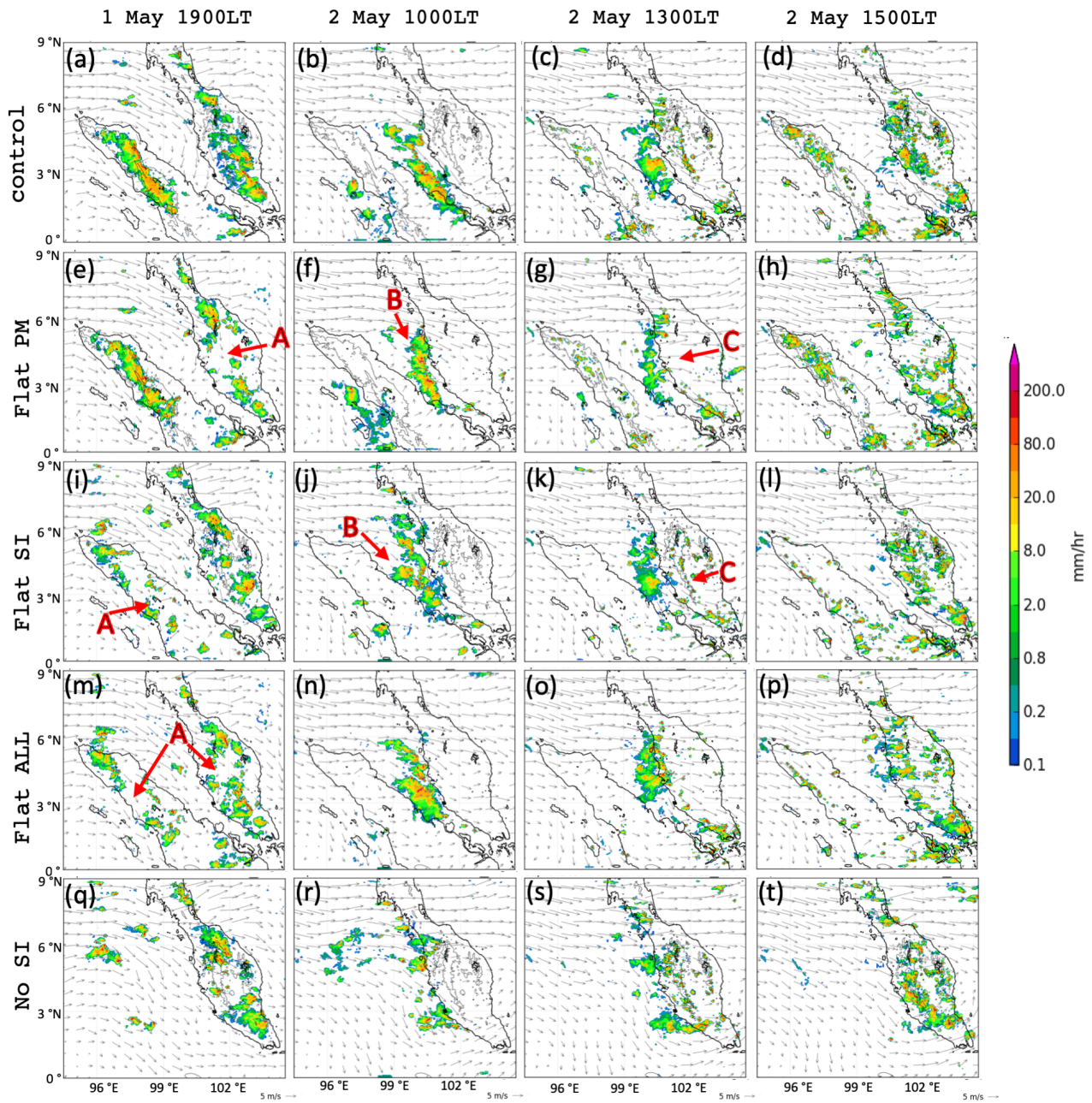
748 FIG. 10. Precipitation and 850hPa winds from the 1.5-km model (CTR) showing the possible mechanisms
 749 for this event. (a) Afternoon rainfall on the 1 May (labeled A and B) provided extra moisture to the region to
 750 produce overnight rainfall over the Strait of Malacca as shown in panel (b). (c) Later, the convection over the
 751 strait and the rainfall in the mountains region over the peninsula influenced the development of rainfall events
 752 over the west coast as shown in panel (d). Grey lines on land masses indicate orography feature of above 500
 753 meters.



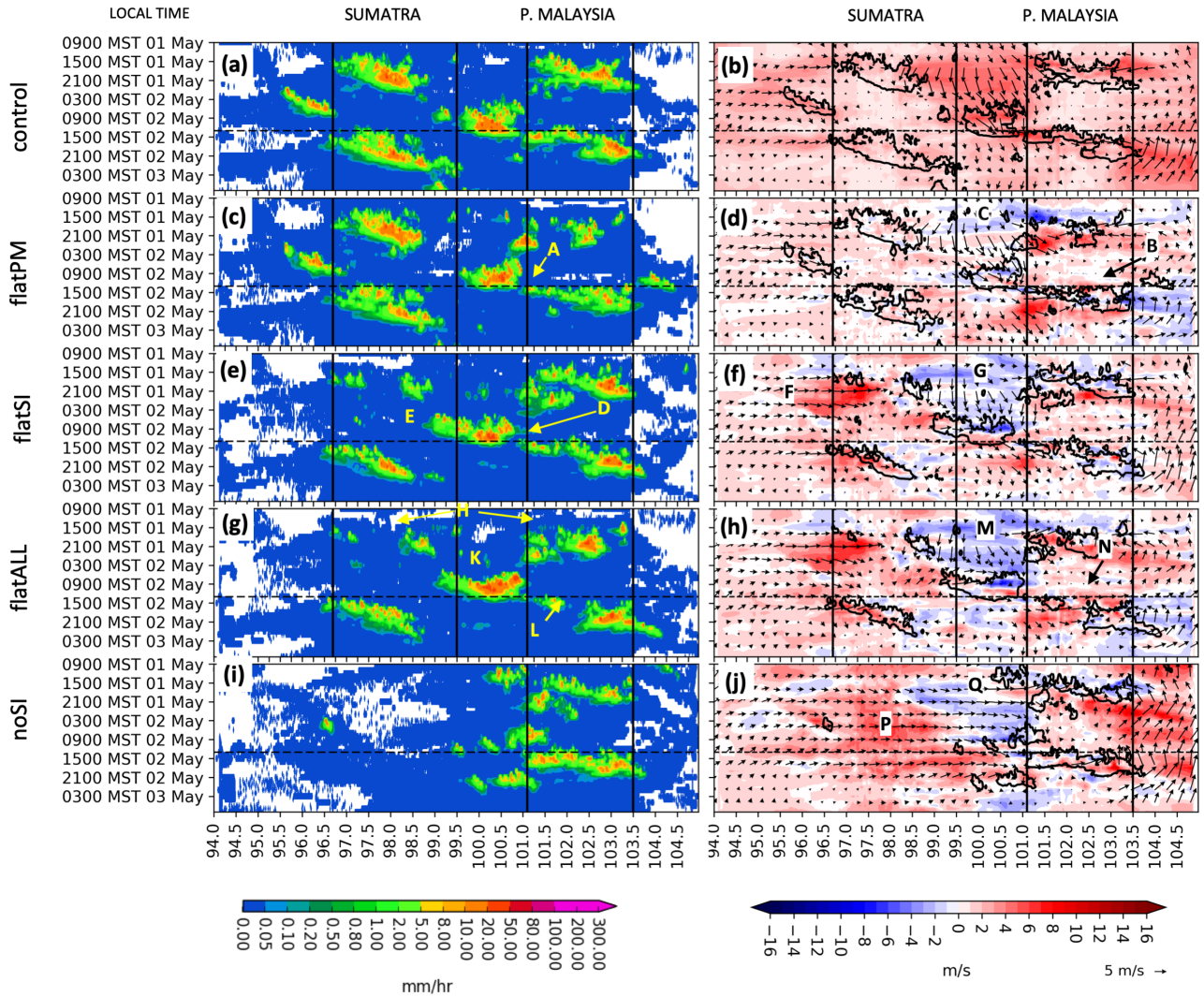
754 FIG. 11. Time-longitude Hovmöller plot, averaged over 3°N to 4°N, of (a) near-surface air temperature
 755 anomaly (21m hybrid level, shaded) and near-surface wind (13 m hybrid level, vectors) averaged over 3°N to
 756 4°N from the 1.5-km model. The red arrows show cold outflows moving toward the center of Strait of Malacca.
 757 The temperature anomaly is the departure from 48-hour mean temperature. (b) near-surface specific humidity
 758 (21m hybrid level, shaded). Red arrows indicate the movement of humidity from both land masses toward the
 759 strait overnight. Black horizontal dashed lines represent the beginning time of the event. Dotted contour line
 760 indicated a 0 °C and 0 kg/kg values, respectively. The y-axis is time in Malaysian Standard Time (MST), 24-hour
 761 format. The x-axis is longitude.



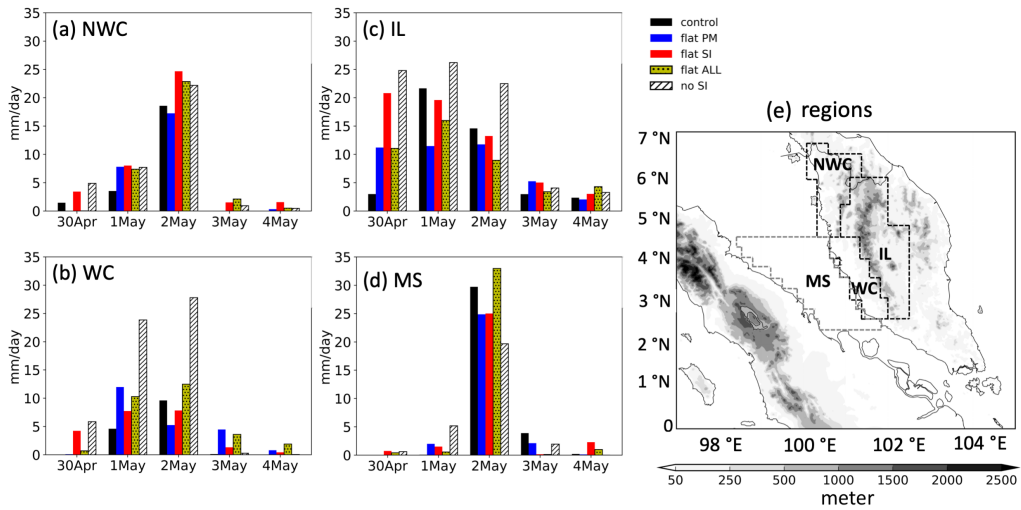
762 FIG. 12. Convergence/divergence plot in the morning of 2 May 2019 from the model simulation showing
 763 where the converging winds were likely to occur. Red-brown color represent converging winds and blue color
 764 represent diverging winds. Dashed black line represent rainfall above 1 mm hr^{-1} . Green arrows represent winds.
 765 All at 13.3 meter model level. Lower right figure shows the plot area.




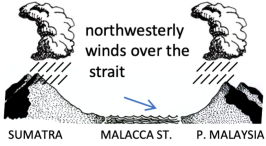

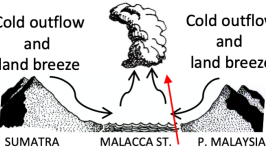

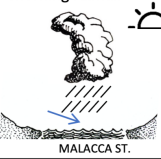
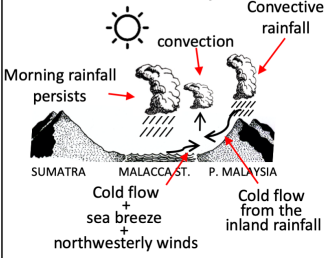

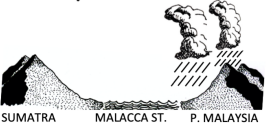
766 FIG. 13. Precipitation and 850hPa winds for comparison between control run, flat Peninsular Malaysia
 767 (**flatPM**), flat Sumatra (**flatSI**), flat Peninsular Malaysia and Sumatra (**flatALL**), and no Sumatra (**noSI**) ex-
 768 periments. The figure compares the main mechanisms in the development of the rainfall on 2 May, in Figure 10.
 769 Grey lines on land masses with no orography modification indicate orography feature of above 500 meters.



770 FIG. 14. Same as in Figure 8a and 9 but for all of the experiments. (a,c,e,g,i) precipitation averaged over 3°N
 771 to 4°N. (b) 233 m wind (vectors) and wind speed (shaded) averaged over 3°N to 4°N. (d,f,h,j) Same as in (b) but
 772 colors represent the wind speed difference from the control run. The same color bar scale is used for both wind
 773 speed and wind speed difference. An additional contour line represents the rainfall above 1 mm hr⁻¹ was added
 774 to the figure. Horizontal black dashed lines indicate the beginning of the event. Panel a and b are for reference
 775 only. The y-axis is time in Malaysian Standard Time (MST), 24-hour format. The x-axis is longitude.



776 FIG. 15. Daily precipitation totals for the three regions of interest: (a) northwest coast, NWC, (b) west coast,
 777 WC and (c) inland, IL. (d) The central region of the Strait of Malacca, MS, and (e) the location of each region.

Mechanisms	Key findings
<p>(a) 2000 MST 1 May </p>  <p>northwesterly winds over the strait</p> <p>SUMATRA MALACCA ST. P. MALAYSIA</p>	<p>i). Both Sumatra and Peninsular Malaysia experienced late afternoon rainfall in the 1 May.</p> <p>ii). Rainfall in 1 May evening occurred in all models run.</p>
<p>(b) 0000 MST 2 May </p>  <p>Cold outflow and land breeze</p> <p>Cold outflow and land breeze</p> <p>SUMATRA MALACCA ST. P. MALAYSIA</p> <p>Convection developed due to cold flow + land breezes and northwesterly winds convergence</p>	<p>i). Cold outflows as a product of the evening rainfall flow toward the Strait of Malacca from both land masses by midnight, in all runs except NoSI.</p>
<p>(c) 0500 MST 2 May</p> <p>Morning rainfall </p>  <p>MALACCA ST.</p>	<p>i). Morning rainfall occurred on 2 May in control, flat PM, flat SI, and flat ALL runs.</p> <p>ii). Morning rainfall in NoSI experiment concentrated closer to the peninsula coast.</p>
<p>(d) 1400 MST 2 May</p>  <p>convection</p> <p>Convective rainfall</p> <p>Morning rainfall persists</p> <p>SUMATRA MALACCA ST. P. MALAYSIA</p> <p>Cold flow + sea breeze + northwesterly winds</p> <p>Cold flow from the inland rainfall</p>	<p>i). In control and flat SI runs: Convection over the western peninsula influenced by rainfall over the strait and sea breeze mechanism, as well as the rainfall over the peninsula from insolation and orographic lifting.</p> <p>ii). In flatPM and flatALL runs: Convection over the western coast influenced by morning rainfall over the strait and sea breeze mechanism over the peninsula (insolation).</p> <p>iii). In NoSI run: convection developed from both convection due to insolation and orographic lifting with possible moister westerly wind.</p>
<p>(e) 1500 MST 2 May</p> <p>developed convective rainfall over the west coast </p>  <p>SUMATRA MALACCA ST. P. MALAYSIA</p>	<p>i). In control, flatSI, NoSI runs: developed rainfall system stay on the west longer as the mountains prevent it to move eastward.</p> <p>ii). In flatPM and flatALL runs: rainfall system moved eastward following the prevailing westerly winds as there are no mountains to prevent.</p>

778 FIG. 16. (left column) Key mechanisms involved in the development of the severe rainfall event over the west
779 coast of Peninsular Malaysia starting from 1 May and on 2 May. The time is in local standard time and a close
780 estimation of when the mechanisms start to occur. (right column) Key findings on the key mechanism in all
781 experiments. (Illustrated by the first author.)